HHS Public Access

Author manuscript

J Neuroimmunol. Author manuscript; available in PMC 2019 March 15.

Published in final edited form as:

J Neuroimmunol. 2018 March 15; 316: 80–97. doi:10.1016/j.jneuroim.2017.12.018.

The neonatal anti-viral response fails to control measles virus spread in neurons despite interferon-gamma expression and a Th1-like cytokine profile

Priya Ganesan[a], **Manisha N. Chandwani**[a], **Patrick S. Creisher**[a], **Larissa Bohn**[a], and **Lauren A. O'Donnell**[a,^]

[a]Duquesne University, Mylan School of Pharmacy, Department of Pharmaceutical Sciences, Pittsburgh, PA 15282

Abstract

Neonates are highly susceptible to viral infections in the periphery, potentially due to deviant cytokine responses. Here, we investigated the role of interferon-gamma (IFNγ), a key antiviral the neonatal brain. We found that (i) IFNγ, which is critical for viral control and survival in adults, delays mortality in neonates, (ii) IFNγ limits infiltration of macrophages, neutrophils, and T cells in the neonatal brain, (iii) neonates and adults differentially express pathogen recognition receptors and Type I interferons in response to the infection, (iv) both neonates and adults express IFNγ and other Th1-related factors, but expression of many cytokines/chemokines and IFNγ-responsive genes is age-dependent, and (v) administration of IFNγ extends survival and reduces CD4 T cell infiltration in the neonatal brain. Our findings suggest age-dependent expression of cytokine/chemokine profiles in the brain and distinct dynamic interplays between lymphocyte populations and cytokines/chemokines in MV-infected neonates.

Graphical Abstract

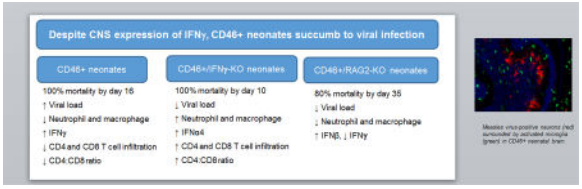

Keywords

interferon-gamma; neonatal; T cells; natural killer cells; microglia; Measles virus

^Corresponding author: Duquesne University, Mylan School of Pharmacy, 441 Mellon Hall, Pittsburgh, PA 15217, Phone: 412-396-5133, Fax: 412-396-4660, odonnel6@duq.edu.

1. Introduction

Infections by neurotropic viruses are among the most common congenital infections in newborns and contribute directly to the development of blindness, hearing loss, cognitive deficits, and epilepsy (Das and Basu, 2011). Further, viral infections in the central nervous system (CNS) are hypothesized to indirectly contribute to neurodegenerative and neuropsychiatric diseases later in life due to damage from a previous infection (*e.g.* schizophrenia, Parkinson's Disease) (Jang et al., 2009, Khandaker et al., 2013, Landreau et al., 2012). While it is clear that many neurotropic viruses are capable of causing significant disease in the neonatal brain, the functionality of the anti-viral immune response and how it contributes to neuropathology in neonates is poorly defined.

Neuronal loss during CNS infections may occur through direct infection and killing of neurons by the virus or through the anti-viral immune response generated against the infected CNS cells. In the brain, a non-cytolytic approach to viral clearance could be favorable for infected neurons, as these cells are largely non-renewable. Lytic approaches to viral clearance, such as through granzymes and perforins, carry the risk of irreversible damage and cell death to the infected neurons, which could contribute to long-term neurological deficits. In many adult models of CNS infection, the pleiotropic cytokine interferon gamma (IFNγ) is key to suppressing viral spread while sparing the infected neurons through non-cytolytic clearance, thus limiting neuropathology and viral replication (Burdeinick-Kerr et al., 2007, Hausmann et al., 2005, Larena et al., 2013, Patterson et al., 2002, Stubblefield Park et al., 2011). However, in neonates, viruses often spread rapidly in brain tissue despite the initiation of an immune response (Hausmann, Pagenstecher, 2005, Kopp et al., 2014, Manchester et al., 1999). This demonstrates the importance of better defining neonatal immune responses within the CNS.

Evidence from peripheral infections shows that the neonatal immune response induces a distinct cytokine profile when compared to an adult response against the same pathogen (reviewed in (Adkins et al., 2004)). Depending upon the type and dose of antigen, neonatal T cells often skew towards a Th2-like response (including production of IL-4, IL-5, and IL-13) as opposed to a Th1 response, characterized by the production of IFNγ and TNF (Zaghouani et al., 2009). During a CNS infection, one could hypothesize that a Th1 response would be preferred in order to ensure adequate IFNγ expression and control viral replication in developing neurons while minimizing neuronal loss. However, IFNγ also has been shown to play both neurotoxic and neuroprotective roles for developing neurons, making the influence of IFNγ in controlling neonatal infections in the brain less clear (Mizuno et al., 2008, O'Donnell et al., 2015).

In the current study, our goal was to examine how IFNγ impacts the neonatal immune response generated against virally-infected neurons. To accomplish this, we used the transgenic CD46+ mouse, which expresses the human isoform of the measles virus (MV) receptor CD46 under the control of the neuron-specific enolase (NSE) promoter (Rall et al., 1997). Thus, human CD46 expression and viral infection are restricted to mature CNS neurons. We evaluated adult and neonatal CD46+ mice lacking IFNγ or lacking adaptive immune cells for the development of an anti-viral immune response against MV-infected

neurons in the brain. We show that IFNγ delays mortality and limits immune cell infiltration into the CNS of neonatal mice, but is insufficient to control viral spread or prevent mortality, despite an associated Th1-like cytokine profile in the brain.

2. MATERIALS AND METHOD

2.1. Animals and ethics statement

Mice were maintained and treated in accordance with the Institutional Animal Care and Use Committee of Duquesne University and the *NIH Guide for the Care and Use of Laboratory Animals*. CD46+, CD46+/IFNγ knockout (KO), and CD46+/Recombination activating gene 2 (RAG-2) KO mice (A gift from Dr. Glenn Rall; Fox Chase Cancer Center, Philadelphia, PA) were maintained on a 12:12 light/dark cycle under controlled temperature conditions (20 ± 2 °C) with free access to food and water. Harem mating cages were established for the CD46+, CD46+/IFNγ KO and CD46+/RAG2 KO mice in order to generate neonatal pups for infections.

2.2 Measles virus infections and IFNγ treatments

Mice were infected with Measles virus (MV)-Edmonston obtained from the ATCC (American Type Culture Collection; Cat. No: VR-24). The virus was passaged twice in Vero fibroblasts. The inoculum was diluted to 10,000 plaque forming units (PFU)/10 μl with phosphate-buffered saline (PBS) prior to injection.

On postnatal day 2 (P2), pups were intracerebrally injected with virus, using a 27½ gauge needle, along the cerebral midline. The uninfected control group was injected in the same location with an equal volume of PBS (10 μl). Pups were monitored daily for symptoms of illness (seizures, tremors and dehydration) and survival, up to 35 days post-infection. Mice were euthanized if seizures developed. Adult mice (3–4 months of age) were anesthesized with isoflurane and injected with 30 μl (30,000 PFU) of MV along the cerebral midline. Infected mice were monitored for signs of illness daily throughout the course of infection. For pups receiving recombinant murine IFNγ, 100U of IFNγ (BD Biosciences) was injected intracranially with the virus at the time of infection. Pups received an interperitoneal injection of IFNγ (100U in 10μl PBS) every three days afterwards until the mice succumbed to the infection.

2.3 Quantitative RT-PCR

Quantitative RT-PCR for measles virus nucleocapsid (N) was performed as described previously (O'Donnell et al., 2012). Mouse brains were snap frozen in liquid nitrogen and stored at −80°C. RNA was isolated by TRIzol, according to the manufacturer's instructions (Sigma-Aldrich). Contaminating DNA was removed from RNA preparations using DNase I treatment (Invitrogen). Purified RNA was quantified using a Nanodrop instrument. RNA was reverse transcribed using Moloney murine leukemia virus reverse transcriptase (Ambion) and a mixture of anchored oligo-dT and random decamers. For each sample, two reverse transcriptase reactions were performed with inputs of 100 and 20 ng. An aliquot of the cDNA was used for 59-nuclease assays using TaqMan chemistry. A TaqMan set specific for the N gene of MV (GenBank sequence AB046218) was used for detecting viral

nucleocapsid RNA. Sequences were as follows: forward, 59-CGCAGGACAGTCGAAGGTC-39; reverse, 59-TTCCGAGATTCCTGCCATG- 39; probe, 59-6Fam-TGACGCCCTGCTTAGGCTGCAA-BHQ1-39. Assays were used in combination with Universal Master mix and run on a 7900 HT sequence detection system (Applied Biosystems). Cycling conditions were 95°C, 15 min, followed by 40 (twostep) cycles (95°C, 15 s; 60°C, 60 s). The assay for MV-N was validated with a 4-fold five-points dilution curve of cDNA. The slope was 23.54, corresponding to a PCR efficiency of 95%. For each sample, the values are averaged and SD of data are derived from two independent PCRs. Relative quantification to the control was done using the comparative cycle threshold method.

For qRT-PCR analysis of the pathogen recognition receptors and interferons, we reverse transcribed RNA using QuantiTect Reverse Transcription Kit (20531, Qiagen) to produce cDNA, then amplified using primers from Integrated DNA Technologies (Coralville, IA). The sense and antisense primer sequences are available upon request (McCarthy et al., 2015, Zalinger et al., 2015). Real time PCR was performed using Bullseye EvaGreen qPCR Mastermix (MIDSCI) on an StepOne Plus qPCR detection system (Thermo Fisher Scientific) using a MicroAmp Fast optical reaction plate (4346906, Applied Biosystems). mRNA was quantified as ΔCT (threshold cycle) values relative to GAPDH. ΔCT values of the infected samples were expressed as fold changes over ΔCT values of control samples.

2.4. Flow cytometric analysis of brain homogenates

At specific days post-infection (dpi), mice were deeply anesthetized with isoflurane. Once the mice were unresponsive, the brain and spleen were removed and pressed through a nylon mesh cell strainer in PBS. The dissociated tissue was run over a 30/70% discontinuous Percoll gradient for 20 min at 4°C. Mononuclear cells were collected from the interface, washed with PBS, treated with 0.84% ammonium chloride to remove contaminating red blood cells (RBCs), and washed again in PBS. Primary antibodies (Abs) were applied in a solution of 1% fetal bovine serum/PBS for multi-color flow cytometry. The following Abs (BD Biosciences) were used to identify T cells: APC CD8a (561093), FITC CD19 (557398), PE CD4 (553048), and PerCP-CY™ 5.5 CD3 Molecular complex (560527). To identify NK cells, APC NK1.1 (55067), PE CD49b (553858), PerCP-CY™ 5.5 CD3 Molecular complex (560527), and FITC CD19 (557398) were used. All antibodies were added at a concentration of 600ng/ml. To identify neutrophils, PerCP CD45 (557235), CD11b APC (eBioscience 17-0112-81), and Ly6G FITC (551460) are used at 1:50 dilution. Microglia and macrophages were distinguished by $CD45^{intermediate}/CD11b^{+}$ and $CD45^{high}/CD11b^{+}$ staining, respectively. Cells were incubated with Ab for 1h at 4°C and then washed with 1% FBS/PBS. Pelleted, stained cells were resuspended and analyzed in a BD Accuri CFlow flow cytometer (BD Biosciences). For each sample, 1×10^5 events were run, with gates to exclude debris and doublet cells. Single antibody stains were used for color compensation and isotype controls were used for gating each immune cell marker. (O'Donnell, Conway, 2012)

2.5. Immunohistochemistry of mouse brain tissue

Neonatal and adult mice were anesthetized and perfused with ice-cold 4% Paraformaldehyde/PBS (PFA/PBS). Brains from MV-infected and mock-infected neonates

and adults were collected and cut along the midline into two halves. The brains were post-fixed with 4% PFA/PBS and cryoprotected with 30% sucrose in PBS at 4°C. Then the brains were immersed in tissue embedding compound (TFM-5, TBS), frozen in a dry ice-isopentane bath, and stored at −80°C. Sagittal cryosections (16 μM) were cut on a cryostat (Microm HM-550, GMI). Standard immunohistochemistry was performed to detect mouse anti-measles hemagglutinin (Millipore MAB8905; 1:200), mouse measles matrix protein (Millipore MAB8910; 1:200), and rabbit anti-ionized calcium-binding adapter molecule 1 (Iba1) (Wako 019-19741; 2μg/ml) for microglia/macrophages overnight at 4°C. Sections were washed (3× in PBS) and incubated with Alexa fluor 488 donkey anti rabbit IgG (Molecular Probes A21206; 1:500), Alexa fluor 555 goat anti-mouse IgG (Molecular Probes A21424; 1:500) secondary antibodies, and Hoechst 33343 stain (Thermofisher; 1 μg/ml) for 1 hour at room temperature in the dark. Sections were imaged using an EVOS epifluorescence microscope at 200× magnification. No primary antibody and isotype controls were performed. For all the histological analyses, at least five sections per brain were examined and at least four mice per experimental group were assessed.

2.6. Western Blot

Adult and neonatal CD46+ mice (7 dpi and age-matched controls) were anesthetized with 3.8% choral hydrate in PBS and perfused with ice-cold PBS with 10mM sodium fluoride as a phosphatase inhibitor. Brains were harvested and dissected for the hippocampus and cerebellum, weighted, and lysed in 1× Cell Lysis Buffer (Cell Signaling Technology, Danvers) with 1x Protease Inhibitor cocktail (Sigma-Aldrich, St. Louis, MO) (20 μl lysis buffer/mg tissue). Protein lysates were stored at −80°C until analysis. The protein concentration of each lysate was measured using the Pierce BCA Protein Assay Kit (Thermo Fisher, New York, NY). For each sample, 20μg of lysate was subjected to sodium dodecyl sulfate–polyacrylamide gel electrophoresis on NuPAGE 4–12% Bis-Tris gels (Life Technologies, Grand Island, NY). The gel was blotted onto Immobilon-FL Membrane (Millipore, Billerica, MA) and the membranes were blocked using a 1:1 mixture of 1X phosphate buffered saline/Tween-20 solution (Sigma-Aldrich, St. Louis, MO) and Odyssey blocking buffer (Licor Biosciences, Lincoln, NE) for 30 min at 20°C. The membranes were treated with primary antibody solutions diluted in a 1:1 mixture of 1X phosphate buffered saline/Tween-20 solution (Sigma-Aldrich, St. Louis, MO) and Odyssey blocking buffer (Licor Biosciences, Lincoln, NE) overnight at 4°C on a rocker. The membranes were washed thrice with PBS-Tween for 10 min each and incubated in secondary antibody solutions (donkey anti-mouse 680, goat anti-mouse 800, goat anti-rat 800 (Licor Biosciences; 1:10000), or goat anti-rat 680 (1:1000; Licor Biosciences) for 60 min at 20°C. The membranes were washed thrice in PBS-Tween and imaged on the Odyssey Infrared Imaging System (Licor Biosciences, Lincoln, NE). Individual bands were quantified using Image Studio software (Licor Biosciences, Lincoln, NE, version 3.1.4). The signal from each band was normalized against the GAPDH signal as a loading control. Primary antibodies used were as follows: rat anti-TLR3 (Novus Biologicals NBP2-27404; 1:250); rat anti-TLR7 (R&D Systems MAB7156; 1:500), rat anti-RIG-1 (BioLegend #635202; 1:500), and mouse anti-GAPDH (Millipore MAB374; 1:25000).

2.7. Cytokine and chemokine gene expression

RNA was isolated from adult and neonatal mouse brains using the Qiagen RNeasy Midi Kit (75124, Qiagen, Valencia, CA). The extracted RNA was assessed by UV spectrophotometry to measure concentration and purity on a Nanodrop (ND-1000, Thermo Scientific). Cytokine and chemokine gene expression was assessed using the mouse cytokine and chemokine RT2 Profiler PCR Arrays (PAMM-150Z, Qiagen) by the manufacturer. The expression of 84 inflammatory genes and 5 housekeeping genes were assessed. Data analysis was done using the SABiosciences RT2 Profiler Web-Based PCR Array Data Analysis software, which automatically performs the Delta Ct (ΔΔCt) fold-change calculations from the uploaded raw threshold cycle data. The fold-change in infected brains as compared to uninfected controls was calculated after normalizing to the housekeeping genes.

2.8. Statistical Analysis

Statistical analysis for the Kaplan-Meier plots was performed by log rank test to compare survival across different genotypes. A two-way ANOVA was performed to compare body weight, brain weight, viral load, NK cell, T-cell, and macrophage/microglial counts, qRT-PCR, and western blot data with Bonferroni post hoc test ($p<0.05$ considered as significant). A one-way ANOVA was performed to compare neutrophil infiltration. For the cytokine/chemokine array and T cell counts from IFNγ-treated mice, p values were calculated based on a student's t-test to compare the control and treatment groups. Differences were deemed significant when p values were less than 0.05. Statistical analysis was performed using GraphPad Prism software (GraphPad Software, Inc., La Jolla, CA) and SPSS.

3. RESULTS

3.1. IFNγ delays, but does not prevent, mortality in infected neonates

To understand the antiviral response in the neonatal CNS, we used the CD46+ mouse model to establish a neuron-restricted measles virus infection in the brain. Immunocompetent CD46+ adult mice initiate a protective adaptive immune response with infiltration of CD4 and CD8 T cells as early as 3 days post-infection (dpi), with peak T cell infiltration between 7–14 dpi. MV infection is resolved typically by 30 dpi without any symptoms or signs of illness (Patterson, Lawrence, 2002). Both T cells and IFNγ are critical to the survival of adult CD46+ mice. CD46+ adult mice lacking mature T and B cells (CD46+/RAG2-KO) experience 100% mortality during infection, whereas CD46+ adult mice lacking only B cells do not succumb to the infection (Solomos et al., 2016). CD46+ adult mice that lack IFNγ (CD46+/IFNγ-KO) do not clear the virus, with ~50% of the mice succumbing to the infection within 21 dpi (O'Donnell, Conway, 2012). In order to study the outcome of infection in neonates, 2-day old CD46+ mice were infected with MV and monitored for signs of illness and mortality over a similar time frame (Figure 1A). As a control for the injection procedure, CD46+ neonates were injected with 10μl of PBS intracerebrally and did not show signs of illness and over the course of the experiment. MV-infected CD46+ neonates succumbed to the virus by 16 dpi, with 50% mortality by 8 dpi. During the infection, MV-infected neonates showed signs of illness including dehydration, lethargy, and tremors starting at 6dpi, with seizure activity before death.

Previous studies have shown that IFNγ-producing T cells are required for MV control in adult CD46+ mice (Lawrence et al., 1999, O'Donnell, Conway, 2012, Patterson, Lawrence, 2002). To determine if IFNγ contributed to the outcome of infection in neonates, CD46+/IFNγ-KO pups were infected with MV and observed for signs of illness (Figure 1A). MV-infected CD46+/IFNγ-KO pups succumb to the infection earlier than CD46+ pups, reaching 100% mortality by 10 dpi. We also investigated the role of the adaptive immune system in neonates using recombinase activating gene 2 knockout mice (CD46+/RAG2-KO). We observed that CD46+/RAG2-KO neonates survive longer than CD46+ and CD46+/IFNγ-KO neonates. At 35 dpi, 20% of CD46+/RAG2-KO neonates had survived the infection with less signs of illness than the other CD46+ genotypes. These observations suggest that the adaptive immune response may play a detrimental role during neonatal infection, in contrast to the protective role that it plays in the adult brain. Furthermore, these findings demonstrate that IFNγ delays the pathogenic outcomes of infection, but is insufficient to protect the CD46+ neonates from death.

3.2 Measles virus RNA is lower in the absence of IFNγ compared to CD46+ neonates

Because CD46+/IFNγ-KO neonates succumb to the infection earlier than CD46+ neonates, one possibility is that MV replication is greater in the absence of IFNγ, thereby leading to more rapid death. To determine if survival correlates with the viral load in the brain, expression of measles virus nucleocapsid (N) RNA was determined in brain tissue using qRT-PCR (Figure 1B and 1C). We focused on 4 and 6 days post-infection, as these time points correspond with early T cell infiltration (4 dpi) and with more extensive T cell infiltration (6 dpi). Regardless of immune background, MV RNA increased in all neonates over time, although this increase was only significant in CD46+ pups ($p<0.001$). Unexpectedly, CD46+ neonates had a higher viral load compared to CD46+/IFNγ-KO ($p<0.05$) and CD46+/RAG2-KO neonates at 6 dpi ($p<0.001$, Figure 1B). Thus, the level of viral RNA did not correlate with survival in the CD46+ neonates (Figure 1A). This result suggests that the virus may not be directly causing death in neonates, but rather the nature of the host immune response may be a better predictor of survival. Regardless of genotype, levels of MV N-transcripts were higher in neonates than in adults (Figure 1C), which may reflect both a more successful anti-viral response in adults and/or the ability of the virus to readily spread in young neurons.

3.3 Impact of MV-infection on body and brain weights

MV-infected neonates develop neurological symptoms, including ataxia and seizures, as well as signs of wasting and dehydration. In ~8% of CD46+/IFNγ-KO neonates, enlarged heads and skulls were observed at the later stages post-infection (8–10 dpi). Upon dissection, edema was observed in the intracranial space, with fluid accumulation in the brain and reduced brain size. In contrast, CD46+ neonates did not demonstrate overt changes in head size during the infection. Thus, we determined if the loss of body weight correlated with changes in brain weight during infection (Figure 2). At the initial stages of infection (2 dpi), there is no difference in the body or brain weight of MV-infected CD46+ (Figure 2A and 2C) or CD46+/IFNγ-KO (Figure 2B and 2D) neonates compared to uninfected controls. As the infection progresses, CD46+ neonates lose body weight at 4 dpi (11.7% loss compared to uninfected controls) followed by a transient increase in body (13.5%) and brain weight

(6.2%; $p<0.05$) at 6 dpi. MV-infected CD46+/IFNγ-KO neonates also show an increase in brain weight at 6 dpi (13%), but there is no difference in body weights compared to control. At 10 dpi, MV-infected CD46+ (loss of 10.3% brain weight; 21% body weight) and CD46+/IFNγ-KO (loss of 14.3% brain weight; 29% body weight) neonates show a significant decrease in brain and body weight compared to age-matched controls. Thus, MV-infected pups showed limited growth at the end stages of infection (10 dpi), when neurological symptoms are also the most severe. The finding that brain weights increased at 6 dpi, regardless of IFNγ expression, was surprising, as neurological symptoms are apparent at this time point. However, one possibility is that the temporary increase in brain weight could be due to edema or increased fluid retention in the tissue at that stage of infection, as the brains were not dried to eliminate water weight before measurement. Regardless of the increase in weight at 6 dpi, the loss of brain and body weights occurred independently of IFNγ, even when edema was not present. The ratios of brain weight/body weight were similar for both CD46+ and CD46+/IFNγ-KO neonates regardless of infection (0.07 for both genotypes) at 6 dpi. However, at 10 dpi, the ratio increases in CD46+/IFNγ-KO neonates (0.1 in infected pups versus 0.05 for uninfected pups), but remains similar in CD46+ neonates (0.06 in infected and uninfected pups). Despite the reduction in brain weights in the absence of IFNγ, there is also a greater reduction in body weights at 10 dpi (Figure 2D), which is indicative of the severity of wasting in the CD46+/IFNγ-KO pups.

3.4. IFNγ limits microglia/macrophage numbers during infection

IFNγ stimulates the activation of microglia and induces expression of chemokines that are mediators of T-cell recruitment (Rock et al., 2005). During brain insults, circulating monocytes migrate to the breached BBB and enter the brain. Thus, both the infiltrating monocytes and microglia contribute to the neuroimmune response in the brain. We hypothesized that pups lacking IFNγ would show limited microglial/macrophage induction during infection. Microglia were identified by $CD45^{intermediate}/CD11b^{+}$ staining and macrophages by $CD45^{high}/CD11b^{+}$ in the brain by flow cytometry (Greter et al., 2015). In CD46+ neonates, we observed that there is no change in the number of microglia from 4 to 6 dpi (Figure 3A). In CD46+/IFNγ-KO and CD46+/RAG2-KO neonatal brains, there is a significant increase in microglial numbers from 4 to 6 dpi ($p < 0.001$). When compared across the genotypes, we observe that CD46+/IFNγ-KO neonates have the highest number of microglia at 6 dpi compared to CD46+ ($p < 0.001$) and CD46+/RAG2-KO neonates ($p < 0.05$). Similar to microglia numbers, neonates without IFNγ showed the highest infiltration of macrophages at 6 dpi (Figure 3B). From 4 to 6 dpi, there is a significant influx of macrophages in CD46+/IFNγ-KO neonates post-infection, whereas CD46+/RAG2-KO neonates showed no change in macrophage numbers as the infection progressed. These findings suggest IFNγ may confer an anti-inflammatory effect in the neonatal CNS, as the numbers of macrophages/microglia were elevated in the absence of IFNγ.

We also examined changes in microglial/macrophage morphology in the brain parenchyma post-infection. Sagittal brain sections were immunostained for microglia/macrophages using Iba1 (green), which is a marker that shows increased expression in activated cells (Sasaki et al., 2001), and for measles virus antigen using antibodies against the matrix and hemagglutinin protein (red, Figure 3). In CD46+ (Figure 3C) and CD46+/IFNγ-KO brains

(Figure 3D), activated microglia/macrophages were observed with bright Iba1 staining in the brain parenchyma in comparison to uninfected controls. MV antigen was observed in the prefrontal cortex, thalamus, and cerebellum at 7 dpi regardless of IFNγ expression. At the later stages of infection (10 dpi), there is widespread MV infection throughout the CNS, including involvement of the hippocampus, which is also highly infected in adults (data not shown). Microglia/macrophages with bright Iba1 staining were consistently observed in close proximity to MV-infected neurons. In brain regions with MV+ cells, Iba1+ cells showed ameboid morphology with rounder cell bodies and retracted processes in both CD46+ and CD46+/IFNγ-KO pups. Iba1+ cells in uninfected brains show thin, ramified processes and with less intense Iba1 staining (Figure 3C and 3D, top rows) in comparison to MV-infected brains. Thus, changes in microglia/macrophage morphology are observed in the absence of IFNγ, suggesting that other cytokines/chemokines can trigger activation during infection.

3.5. IFNγ does not affect natural killer cell infiltration, but limits neutrophil infiltration into the CNS

Natural killer (NK) cells play an important antiviral role by direct lysis of infected cells and/or release of antiviral cytokines such as IFNγ, particularly during early stages of infection before a specific adaptive response is mounted (Biron et al., 1999, Paolini et al., 2015). Since NK cells can be major producers of IFNγ, we investigated whether NK cells infiltrate into the brain parenchyma in neonates. As NK cells are part of the innate immune response, we quantified the early stages of infection (2 and 4 dpi) as well as a time point where T cell infiltration was increasing (6 dpi) (Figure 4). At 2 and 4 dpi, there is no significant difference in MV-infected pups compared to uninfected controls regardless of IFNγ expression. At 6 dpi, there is a significant increase in total NK cell number (NK1.1+, CD49b+, and NK1.1+/CD49b+) in MV-infected neonates compared to uninfected controls in both CD46+ (Figure 4A $p<0.05$) and CD46+/IFNγ-KO (Figure 4B, $p<0.001$) genotypes. Collectively, this data show that NK cells arrive in the CNS during infection independently of IFNγ.

We next investigated whether IFNγ affects neutrophil infiltration. Neutrophils are recruited early in viral infections, and can contribute to tissue damage through protease and oxidase release during viral clearance (Drescher and Bai, 2013). Neutrophils are also capable of producing IFNγ in response to various pathogens (Sturge et al., 2013). In neonates that lack IFNγ, neutrophil ($CD45^{hi}$, CD11b+, and Ly6G+) infiltration is significantly higher compared to CD46+ neonates at 4 and 6 dpi (Figure 4C). CD46+/RAG2-KO neonates also show progressively elevated levels of neutrophils in the CNS, but it is not significantly different from CD46+ or CD46+/IFNγ-KO neonates at either time point. This suggests that IFNγ may downregulate neutrophil recruitment in the CD46+ neonates during infection, and that excessive neutrophil infiltration may correlate with earlier death in CD46+/IFNγ-KO neonates.

3.6. Higher infiltration of neonatal T cells in the absence of IFNγ at later stages of infection

Studies by Solomos and colleagues suggest that CD4 T cells, in conjunction with CD8 T cells or B cells, are required for viral control in CD46+ adults (Solomos, O'Regan, 2016).

Furthermore, T cell infiltration correlates with IFNγ expression in the CD46+ adult brains ((O'Donnell, Conway, 2012). Thus, we investigated the infiltration of T cells in neonatal brains after MV infection. Using flow cytometry of whole brain homogenates, the numbers of CD4 and CD8 T cells in the neonatal brain were quantified at 4, 7, and 10 dpi, which corresponds to time points where T cells are first observed by immunohistochemistry (4 dpi) and time points that parallel peak infiltration of T cells in adults (7 and 10 dpi). At 4 dpi, there is no difference in the number of CD4 or CD8 T cells in the infected CD46+ neonates compared to uninfected controls (Figure 5A and 5B). There is higher infiltration of CD4 T cells in the absence of IFNγ early in infection at 4 dpi (Figure 5A). Similarly, at 7 dpi, significant CD4 T cell infiltration was observed only in the absence of IFNγ (Figure 5C), whereas CD8 T cell infiltration was induced in MV-infected neonates regardless of IFNγ expression (Figure 5D). At later stages of infection (10 dpi), significant infiltration of CD4 (Figure 5E) and CD8 T cells (Figure 5F) was observed only in the CD46+/IFNγ-KO pups in comparison to uninfected controls. CD46+ pups did not show a significant increase in CD4 or CD8 T cells at 10 dpi, although a trend toward increasing CD8 T cell number was observed ($p=0.082$). Comparing across genotypes, CD46+/IFNγ-KO neonates have significantly higher infiltration of CD4 T cells ($p<0.001$) and CD8 T cells ($p<0.05$) compared to CD46+ neonates at 10 dpi. Thus, these results suggest that IFNγ may have a suppressive/anti-inflammatory effect on T-cell infiltration at later time points in infection.

3.7. Greater CD4 T cell infiltration in adults compared to neonates regardless of IFNγ expression

We next determined whether there were age-dependent differences in the number of T-cells infiltrating into the brain (Figure 6). CD46+ and CD46+/IFNγ-KO adults have a significantly higher number of CD4 T cells compared to neonates of both genotypes in infected whole brain tissue (Figure 6A, $p<0.05$). CD8 T cells in CD46+/IFNγ-KO adults are significantly higher compared to MV-infected neonates (Figure 6B, $p<0.05$). However, in the CD46+ genotype, there is no difference in the number of CD8+ T cells between adults and neonates. Additionally, in contrast to the neonates, there is no difference in the T cell numbers between CD46+ and CD46+/IFNγ-KO adults. We also compared the CD4:CD8 T cell ratio in adults and neonates. CD46+ adults (5.9), CD46+/IFNγ-KO adults (2.6), and CD46+/IFNγ-KO neonates (2.9) were skewed towards CD4 T cells. Whereas CD46+ neonates (0.5) have a ratio that is skewed towards CD8 T-cells. Of note, only CD46+ adult mice can control MV in the CNS (O'Donnell, Conway, 2012). This suggests that CD46+ neonates and the CD46+/IFNγ-KO mice lack adequate CD4+ T cell helper function, which may contribute to the relatively high viral load and poor pathological outcome.

3.8. CD46+ neonates and adults differentially express PRRs and Type 1 interferons during infection

As we observed greater T cell infiltration in the adults despite a lower viral load than the neonates, we considered the possibility that enhanced expression of pattern recognition receptors (PRRs), and subsequent Type I IFN expression, could correlate with the relatively robust immune response that is eventually induced in adults. Recognition of viral RNA by PRRs such as the cytoplasmic retinoic acid-induced gene-I (RIGI) and the membrane bound Toll-like receptors (TLRs) lead to the induction of Type 1 IFNs, which are significant early

steps in viral control (Akira et al., 2006, Yoneyama et al., 2004, Zalinger, Elliott, 2015). For our analysis, we focused on RIGI, which is expressed in the brains of MV-infected transgenic mice expressing Hsp70, and TLR 3 and 7, which recognize viral RNAs (Kim et al., 2013, Sorgeloos et al., 2013). TLR3, in particular, has been shown to be induced by the MV-Edmonston strain in cell lines (Tanabe et al., 2003). During infection of CD46+ mice, both CD46+ and CD46+/RAG2-KO neonates upregulate RIGI mRNA (12.2-fold and 24.4-fold respectively, Figure 7A) in the brain, whereas infected CD46+ adults did not demonstrate significant upregulation of RIGI mRNA with infection (Figures 7B). CD46+ MV-infected neonates show significantly higher expression of RIGI mRNA compared to CD46+ adults (Figure 7B). CD46+ neonates did not upregulate either TLR3 or TLR7 mRNA (Figure 7E and 7I), while CD46+/IFNγ-KO neonates upregulated TLR3 mRNA (41-fold; Figure 7E) and CD46+/RAG2-KOs upregulated TLR7 mRNA (11-fold; Figure 7I). In contrast, CD46+ adults upregulate TLR3 mRNA (2.3×10^5-fold) and TLR7 mRNA (37.3-fold) to a greater extent than the any genotype of the MV-infected neonates (Figure 7F and 7J). These results suggest that the CD46+ adult mice may rely on the TLR family of proteins for recognition of the virus.

To confirm the mRNA results from whole brain lysates, we examined protein levels of these PRRs in the hippocampus and cerebellum, two brain regions that show high levels of viral infection in neonatal mice. In accordance with the whole brain mRNA, RIGI protein was upregulated with infection in both the hippocampus and cerebellum of infected neonates (22-fold and 15.6-fold versus infected CD46+ adults respectively, Figure 7C and 7D). In contrast with the whole brain mRNA findings, TLR3 protein was not significantly upregulated by adults or neonates in either brain region (Figure 7G and 7H). Additionally, TLR7 protein was upregulated only in the infected CD46+ neonatal cerebellum (6.3-fold) versus uninfected controls (Figure 7L) and not in the hippocampus (Figure 7K). These findings suggest that changes in whole brain mRNA do not necessarily correlate with protein expression in brain regions that carry a high viral load, particularly in adult CD46+ mice, which experience restricted “hot spots” of viral replication in the brain. Moreover, these results imply that neonates, but not adults, induce RIGI expression in the brain tissue during infections.

PRR signaling can trigger the expression of Type I IFNs. Gene expression of the PRRs is further enhanced by elevated IFN expression, allowing for a greater detection of invading pathogens (Schneider et al., 2014). Given the differential expression of PRRs observed in the CD46+ mice, we reasoned that there may be age-dependent differences in the expression of the Type 1 IFNs. Early in infection (3 dpi), we did not observe significant expression of IFNα4 or IFNβ in the adults or neonates of any CD46+ genotype (Figure 8). As the infection progressed (7 dpi), CD46+/IFNγ-KO neonates upregulated IFNα4 (29-fold) to a greater extent in comparison to CD46+ (7.5-fold) and CD46+/RAG2-KO (5.7-fold) neonates post-infection, whereas CD46+ adults did not increase the expression of IFNα4 significantly (Figure 8A, 8B). In contrast, CD46+/RAG2-KO neonates demonstrated greater upregulation of IFNβ in comparison to other neonates (1644.8-fold; Figure 8C). Although IFNβ also was upregulated in the CD46+ neonates (122-fold) at 7 dpi, CD46+ adults did not show significant upregulation of IFNβ at either time point (Figure 8D). We also analyzed levels of the IFN-responsive gene (ISG), Melanoma Differentiation-Associated protein 5 (MDA5),

which is a PRR, as a surrogate for Type I IFN signaling. MDA5 was not induced significantly in infected CD46+ neonates or adults at either time point. At 7 dpi, only the CD46+/IFNγ-KO neonates significantly upregulated MDA5, which may correlate with the elevated IFNα4 observed at this time point. Although it is possible that other IFNα isoforms are expressed in the infected adults, these results suggest that gene expression of Type I IFN and associated ISGs remain relatively low at the start of infection in both neonates and adults, when Type I IFN expression would be expected to dominate. Thus, we propose that the less effective immune response in neonates is not attributable to a diminished Type I IFN response.

3.9. MV-infected neonates upregulate Th1 cytokine and chemokine genes in the CNS

Although Type I IFN expression was not deficient in CD46+ neonates when compared to adults, another possibility is that the cytokine profile produced by the infiltrating neonatal immune cells is not appropriate for viral control. We hypothesized that neonates may express a Th2-biased cytokine response in the CNS, as has been noted in many peripheral infections (Lambert et al., 2014) and could contribute to ineffective viral clearance. To address this question, we examined the mRNA expression of 84 cytokine and chemokines genes in the MV-infected adult and neonatal brains using a qRT-PCR array. Table 1 lists genes that were significantly upregulated by ≥2 fold in the MV-infected neonates and adults compared to age-matched, uninfected controls. Classical Th2 cytokines such as IL-4, IL-5, and IL-13 were not upregulated in either MV-infected neonates or adults. Rather, many Th1-associated cytokines were expressed in comparison to uninfected controls at both ages ($p < 0.05$; Table 1, top panel). Among the Th1-associated factors, IFNγ (11-fold in neonates, 8-fold in adults), IL-1β (3-fold in adults and neonates) and chemokine (C-X-C motif) ligand 10 (Cxcl10; 85-fold in neonates, 44-fold in adults) were upregulated during MV infection at both ages. The anti-inflammatory cytokine interleukin-1 receptor antagonist (IL1rn) is also upregulated in both neonates (17.84-fold) and adults (14.4-fold) post-infection, as well as the expression of several other chemokines genes (Ccl12, Ccl3, Ccl4, Ccl5, Cxcl11 and Cxcl13). These findings suggest that the expression of many inflammatory genes is age-independent in the brain.

Neonates and adults also upregulate unique subsets of genes in an age-dependent manner during infection (Table 1, middle and bottom panel). The expression of tumor necrosis factor (TNF) is significantly increased in MV-infected neonates, but not in adults. Interleukin 10 (IL-10), a global suppressor of the immune response (Moore et al., 2001), was the only Th2-related cytokine to be upregulated in MV-infected neonates. CCL2, which is associated with reduced microglial/macrophage activation in adult infection with mouse hepatitis virus (MHV), (Trujillo et al., 2013) is elevated only in infected neonates (Table 2). MV-infected adults also expressed unique inflammatory genes that were not activated in the neonates. Adult mice show increased expression of the IFNγ-inducible gene CXCL9 (17.67-fold) (Brice et al., 2001), which suggests that IFNγ-responsive gene expression may be partially dependent on age. Of note, gene expression in uninfected neonates and adults revealed modest baseline differences in the absence of infection (Supplemental Table 1). For example, adult mice expressed higher baseline levels of IL-12a (3.98-fold), IL-17a (2.13-fold), and IL-2 (2.13-fold) in the brain than uninfected neonates. Of these cytokines, IL-12a

was the only factor to be upregulated by the neonates upon infection (7.87-fold versus uninfected neonates, Table 1). Together, this data suggests that the majority of cytokines/chemokines that are induced upon infection are distinct from factors that show an age-dependent difference in uninfected controls.

To address differences in survival between the immunocompetent and immunocompromised neonates, we also explored cytokine/chemokine expression in CD46+, CD46+/IFNγ-KO and CD46+/RAG2-KO neonatal brains (Table 2). CD46+/IFNγ-KO and CD46+/RAG2-KO neonates expressed unique subsets of genes that were not upregulated in the immunocompetent CD46+ mice. CD46+/IFNγ-KO neonates upregulated CXCL1 in the brain, which can act as a neutrophil chemoattractant and may partially explain the greater neutrophil infiltration observed in these mice (Figure 4) (Bozic et al., 1995). Surprisingly, CD46+/IFNγ-KO neonates also upregulated CXCL9, which is classified as an IFNγ-inducible gene, suggesting that IFNγ-independent pathways may also regulate CXCL9 expression in the CNS. The CD46+/RAG2-KO neonates, which demonstrated less mortality during infection, activated a number of genes that were not observed in the other neonates (Table 2, **bottom panel**). Various cytokines (IL-5, IL-7, IL-15, and bone morphogenic proteins (BMP) 2, 4, 6, and 7) and chemokines (CCL11, CCL17, CCL19, CCL22, CXCL16) were induced only in CD46+/RAG2-KO brains upon infection. However, comparison of the baseline gene expression between uninfected neonates demonstrates that CD46+/RAG2-KOs have lower basal expression of some of the factors that are upregulated during infection (*e.g.* the BMPs, CCL11, and CCL17; Supplemental Table 2) in comparison to the uninfected CD46+ neonates. Thus, although the CD46+/RAG2-KO neonates express many unique genes upon infection, a subset of these genes are expressed endogenously at low basal levels.

As was seen in the CD46+ neonates and adults, there was overlap in the expression of some Th1-related factors in the neonatal mice. CXCL10 showed the greatest induction in all infected neonates: CD46+ (84.6-fold), CD46+/IFNγ-KO (291.4-fold) and CD46+/RAG2-KO neonates (771.1-fold). IFNγ is upregulated in the CD46+ (11.1-fold) and CD46+/RAG2-KO neonates (15.0-fold), suggesting that innate immune cells are contributing to IFNγ production the absence of T cells. With the exception of IL-10, genes that were activated in the CD46+ neonates but not in the CD46+ adults (Table 1, middle panel) also were expressed in CD46+/IFNγ-KO and CD46+/RAG2-KO neonates. For example, TNF is upregulated in CD46+ (8.4-fold), CD46+/IFNγ-KO (17.9-fold) and CD46+/RAG2-KO (72.1-fold) neonates, but there is no upregulation in the adults. In addition, genes that were only expressed in the CD46+ adults when compared to CD46+ neonates (*e.g.* CXCL9, CCL11; Table 1, bottom panel) were all expressed in the CD46+/RAG2-KO neonates upon infection. Thus, the CD46+/RAG2-KO neonates express a cytokine profile that includes factors that are controlled in an age-dependent manner in the immunocompetent CD46+ mice.

3.10. IFNγ induction occurs independently of age, but activation of the IFNγ-responsive gene CIITA occurs only in adults

To confirm the results of the RT array, we examined the mRNA induction of IFNγ in brain tissue through qRT-PCR at 7 dpi. Expression of IFNγ mRNA was higher in CD46+ neonates

compared to CD46+/RAG2-KO neonates (Figure 9A). Induction of IFNγ mRNA was also greater in CD46+ neonates than in adults (Figure 9B). While we had observed the induction of some IFNγ-responsive genes in both age groups (Table 1), adult mice also expressed IFNγ-responsive genes that were not expressed in neonates (*e.g.* CXCL9), suggesting that neonatal mice may have impaired IFNγ signaling. To investigate the downstream effects of IFNγ signaling, we compared the mRNA expression of CIITA (Class II Major Histocompatibility Complex Transactivator), a critical regulator of MHC-II induction and a IFNγ-responsive gene (Reith et al., 2005). There was no difference in CIITA expression among the three genotypes of the neonates (Figure 9C), despite the expression of IFNγ in CD46+ (11.5-fold) and CD46+/RAG2-KOs (4.4-fold) neonates. However, CD46+ adults induced greater CIITA expression (11-fold) compared to uninfected controls and compared to infected CD46+ neonates (Figure 9D), despite less expression of both IFNγ and MV. These results suggest that although IFNγ may be induced in the brain during infection, there may be deficiencies in IFNγ signaling or transcriptional activation in the neonatal brain.

3.11. IFNγ delays neonatal mortality and reduces CD4 T cell infiltration into the CNS

Finally, although IFNγ is expressed in neonates, we considered the possibility that IFNγ levels may not be sufficient to overcome the relatively high viral load that is found in comparison to the adults. We treated neonatal mice lacking IFNγ with repeated injections of recombinant IFNγ at the start of infection and every 3 days thereafter until the mice succumbed to the infection. CD46+/IFNγ-KO neonates treated with IFNγ showed prolonged survival in comparison to untreated CD46+/IFNγ-KO neonates, although the IFNγ-treated mice ultimately succumbed to the infection (Figure 10A; $p<0.01$ by Log-rank test). As we had observed limited immune cell infiltration in neonatal mice lacking IFNγ, we examined the levels of infiltrating T cells into the CNS with IFNγ treatment at 7 dpi, which is when we first observed a divergence in the survival curves of IFNγ-treated and untreated mice. The numbers of CD4 T cells in the brain was reduced with IFNγ treatment (Figure 10B), while CD8 T cells numbers were unchanged (Figure 10C). These results suggest that IFNγ exerts an anti-inflammatory effect in neonates that limits infiltration of some immune cells and prolongs survival during viral infections in the brain.

4. Discussion

In this study, we demonstrated that the neonatal immune response mirrors many facets of a successful adult response in the brain, including infiltration of multiple innate immune cells and CD4 and CD8 T cells, as well as IFNγ production. Regardless, CD46+ neonates succumb to infection despite mounting a Th1-like, but apparently defective, inflammatory response. Our findings are consistent with the observation that neonatal immune responses are often ineffective at controlling viruses and other pathogens (reviewed in (Rouse and Sehrawat, 2010). However, our findings also contrast with many studies of neonatal peripheral infections, which suggest that a Th2-like bias (with IL-4 and IL-5 expression) predominates during anti-microbial responses (Adkins, Leclerc, 2004, Zaghouani, Hoeman, 2009).

We characterized the role of the Th1 cytokine IFNγ during a neonatal immune response in the brain because IFNγ is indispensable for neuronal clearance of many different viruses (Burdeinick-Kerr, Wind, 2007, Chesler et al., 2004, Komatsu et al., 1996, Larena, Regner, 2013, Patterson, Lawrence, 2002). However, it is important to note that IFNγ also plays both pro- and anti-inflammatory roles in a variety of pathological conditions (Muhl and Pfeilschifter, 2003), in addition to roles in host defense. We reasoned that IFNγ may be protective in the developing CNS during an infection, where neurogenesis and synaptic refinement are active. We have previously shown that IFNγ protects the neural stem cell pool, but does not preserve neurogenesis, in MV-infected CD46+ neonates (Fantetti et al., 2016), suggesting that IFNγ can prevent neural stem loss but cannot prevent loss of function. In the current study, CD46+ pups lacking IFNγ succumb earlier to the infection despite greater infiltration of macrophages, neutrophils,T cells and higher microglial numbers than wildtype pups, which highlights the pleiotropic nature of this cytokine in influencing both leukocyte and neural cell activity. Our findings are also consistent with models of experimental autoimmune encephalitis and sindbis virus infection, where mice deficient in IFNγ signaling demonstrate more severe inflammation and T cell infiltration in the CNS (Lee et al., 2013, Willenborg et al., 1999). Therefore, it is possible that IFNγ plays a protective role by limiting inflammation in the brain during an infection, which is supported by our observation that IFNγ treatment limited CD4 T cell infiltration and prolonged survival (Figure 10).

Multiple studies have shown that neonates have poor Th1 function and a strong Th2 response during microbial infections (Basha et al., 2014, Forsthuber et al., 1996, Powell and Streilein, 1990, Singh et al., 1996). This Th2 bias may be due to delayed maturation of accessory cells or intrinsic epigenetic factors in neonatal T cells. (Li et al., 2004). Th2-like responses are not typically associated with IFNγ production, which is a hallmark of Th1 responses (Schoenborn and Wilson, 2007). Given the significance of IFNγ in viral control in neurons, we predicted that the failure of CD46+ pups to control MV would be due to a Th2-bias in the brain. In neonates, we observed greater induction of IFNγ in response to infection as well as the induction of some IFNγ-responsive genes (CXCL10, CXCL11). However, it is important to note that neonatal CD46+ mice failed to activate CXCL9 and CIITA (Table 1 and Figure 9), both of which are IFNγ-inducible genes, despite greater induction of IFNγ than adults. These findings suggest that IFNγ signaling may be limited in the neonatal CNS, at least in regard to the profile of genes that are activated. Previous studies in CD46+ neonates demonstrate elevated expression and activation of Signal transducer and activator of transcription 1 (STAT1), the canonical signaling molecule downstream of IFNγ, in the hippocampus during infection (Fantetti, Gray, 2016). However, both Type I and II interferons signal through STAT1, so it is possible that STAT1 activation in neonates does not reflect robust IFNγ signaling *per se* at 7 dpi, when Type I IFNs are also expressed. Regardless of the level of STAT1 activation, the disparity in the activation of IFNγ-inducible genes suggests that the outcomes of IFNγ signaling may be dictated by age-related factors.

CD46+/IFNγ-KO neonates, which had the highest levels of immune cell infiltration amongst the neonatal genotypes, succumbed to the infection sooner than neonates expressing IFNγ. The greater infiltration of neutrophils may contribute to the earlier death

observed in the absence of IFNγ, as neutrophil activation during viral infections can lead to tissue damage (Drescher and Bai, 2013, Stout-Delgado et al., 2009). C57BL/6 mice infected with influenza A virus require IFNγ to modulate neutrophil activity in the lung and prevent tissue pathology (Stifter et al., 2016). Thus, the heightened numbers of neutrophils, along with a lack of modulation of neutrophilic activity by IFNγ, may play role in neuropathology in the CD46+/IFNγ-KO neonates. Greater numbers of macrophages/microglia were also noted in the absence of IFNγ, which could contribute to pathology by the release compensatory cytokines (Ottum et al., 2015). Another possibility is that the expression of IFNγ limits T cell infiltration into the brain, thereby limiting cytotoxicity but also allowing for greater viral replication in CD46+ neonates. Previous studies in respiratory syncytial virus (RSV)-infected neonates demonstrate that IFNγ expression or administration in the lung leads to reduced recruitment of CD4 and CD8 T cells (Empey et al., 2012). Thus, a lack of IFNγ expression may allow for greater recruitment of immune cells into the CNS in CD46+/IFNγ-KO neonates, thereby contributing to greater immunopathology and earlier death. Together, these studies suggest that neonatal expression of IFNγ during a viral infection confers an anti-inflammatory effect, which limits T cell recruitment and tissue damage.

The delay in mortality of the CD46+/RAG2-KO neonates with low viral load lends support to the idea that the neonatal T cell response may contribute to neuropathology. Although, the mechanism of protection in the CD46+/RAG2-KO mice requires further study, these findings suggest that the lack of adaptive immune response may be beneficial to survival in the infected neonates. Other models of viral CNS infections, including some strains of west nile virus and dengue virus, show that the CD8 T cell response induces immunopathology while also providing protection against the virus (An et al., 2004, King et al., 2007). Cytotoxic T cells also play a more pathogenic role during infections with Murray Valley encephalitis virus, where mice lacking granule exocytosis showed prolonged survival (Licon Luna et al., 2002). Of note, while providing evidence for a detrimental role for T cell activity during a CNS infection, these studies were performed in adult mice, which contrasts with findings in the adult CD46+ model where viral control is not associated with immunopathology. The CD46+/RAG2-KO neonates were capable of expressing IFNγ during infection, which also suggests that other immune cells, such as neutrophils, were able to compensate for the lack of T cells through expression of key cytokines. A separate, but not mutually-exclusive explanation for the protection observed in CD46+/RAG2-KO neonates is the robust induction of IFNβ. In studies of neonatal mice lacking the type I IFN receptor (IFNAR−/−), MV infection in the CNS was associated with greater mortality than in wildtype neonates (Kim, Shu, 2013). However, although primary neurons can express IFNβ, exposure to IFNβ alone is insufficient to prevent MV replication in neurons (Cavanaugh et al., 2015). Thus, one possibility is that elevated IFNβ expression leads to activation of innate immune cells in the brain, which could subsequently contribute to the reduced mortality seen in CD46+/RAG2-KO neonates.

Adult CD46+ mice depend upon CD4 T cells in concert with CD8 T cells or B cells in order to survive a CNS infection with MV (Solomos, O'Regan, 2016, Tishon et al., 2006). The deletion of CD4 T cells alone results in death of adult CD46+ mice, whereas depletion of CD8 T cells is associated with less viral control but no changes in survival (Solomos,

O'Regan, 2016). Within the adult brain, the CD4:CD8 T cell ratio revealed a greater proportion of CD4 T cells (5.9; Figure 8). In C57BL/6 mice, which are the background strain of the CD46+ model, the CD4:CD8 ratios are relatively low in the spleen, as we also observed in splenocytes from the CD46+ adult mice (1.7; data not shown) (Myrick et al., 2002). During some viral infections, the CD4:CD8 ratio reverses to a greater proportion of CD8 T cells, where the CD8 T cells become necessary for viral clearance either through cytolytic or non-cytolytic mechanisms (Callan et al., 1996, Tripp et al., 1995). The high CD4:CD8 ratio in the adult CD46+ brains, where viral clearance is successful, may suggest that a greater proportion of CD4 help is required to respond to neuronal infections non-cytolytically. These observations in MV-infected adult mice contrast with our findings in CD46+ pups, where the CD4:CD8 ratio skewed toward CD8 T cells (Figure 7). One possibility is that the low proportion of CD4 T cells does not provide sufficient stimulation to the CD8 T cells to produce a non-cytolytic response. Support for this idea is found in a model of neurotropic mouse hepatitis virus infection, where depletion of CD4 T cells impaired the anti-viral function and survival of infiltrating CD8 T cells (Phares et al., 2012). Thus, it is possible that the lack of adequate number of CD4 T cells in neonates may lead to inefficient activation of effector CD8 T-cells and a lack of viral clearance.

Although CD46+ neonates and adults upregulated similar Th1 cytokines and chemokines in the CNS, the expression of some cytokines during infection was age-dependent. Neonatal mice express the anti-inflammatory cytokine IL-10, which is classically associated with Th2-like responses and repression of Th1 cytokine synthesis (Couper et al., 2008). In the CNS, recombinant expression IL-10 is protective against virally-induced demyelination and lymphocyte infiltration (Trandem et al., 2011a). Endogenous IL-10 also protects against neuropathology caused by coronaviruses and flavivirues in murine models of adult infection (Trandem et al., 2011b, Tun et al., 2014). However, the lack of IL-10 induction in CD46+ adult mice suggests that IL-10 is dispensable for non-cytolytic viral clearance from neurons. Similarly, CD46+ neonates, but not CD46+ adults, upregulated TNF during infection. TNF is associated with neuroprotection in models of flavivirus encephalitis (Hayasaka et al., 2013, Tun, Aoki, 2014). Thus, it is surprising that both IL-10 and TNF would be expressed in the neonatal CD46+ model, where viral clearance fails and neuronal dropout is apparent, but not in the adult CD46+ model, where viral control is successful. One possible explanation is that IL-10 induction in neonates dampens the expression of necessary anti-viral or neuroprotective cytokines but does not completely inhibit them, which may explain the extensive overlap in cytokine profiles between adults and neonates despite disparate outcomes in viral control and survival.

Age-dependent innate immune responses may also contribute to early viral control, even if innate immunity is not responsible for the ultimate resolution of the virus. Previous studies indicate that murine neonatal intestinal epithelial cells fail to express TLR3 in response to rotavirus infection through post-natal days 1–10, which overlaps with the time points reflected in our study (Pott et al., 2012). Similarly, human cord blood samples do not induce TLR3 in response to poly(I:C) treatment or HSV activation in comparison to adult NK cells (Slavica et al., 2013). In our model, we observed upregulation of TLR3 mRNA in CD46+ adults but not in CD46+ neonates, although TLR3 protein expression in the adult cerebellum and hippocampus did not reflect the changes in whole brain mRNA. In these brain regions,

we have seen robust MV infection in the neonates; however, this is not consistently the case in the adult brains, where viral spread is more controlled. Thus, it is possible that the brain regions chosen for protein studies in adults did not always carry sufficient virus to stimulate protein expression of the TLRs. Although, we observed robust RIGI expression in the CD46+ neonates, there is also evidence in human neonatal dendritic cells that RIGI function is impaired and associated with attenuated control of RSV (Marr et al., 2014). Despite the varied expression of neonatal PRRs in our model, MV infection was associated ultimately with Type I IFN expression, albeit at a later time point during infection (7 dpi). Sindbis infection in neonatal mice is associated with robust Type I IFN expression, but the mice succumb to the infection regardless, much like the CD46+ neonates (Ryman et al., 2007). In contrast, RSV, LaCrosse virus (LACV), chikungunya virus (CHIKV) infections are associated with less robust Type I IFN responses that also fail to control the virus (Marr, Wang, 2014, Rudd et al., 2012, Taylor et al., 2014). CD46+ adult mice that are deficient in IFNAR demonstrate that Type 1 IFN signaling contributes to early viral control, but is dispensable for the ultimate resolution of the virus (Cavanaugh, Holmgren, 2015). As we did not observe significant upregulation of the Type I IFNs in CD46+ adults, we suspect that Type I IFN is undetectable in whole brain RNA because the expression may be restricted to regions of viral replication, which are relatively limited in the adult brain. Thus, while Type I IFN expression is invoked in many neonatal infection models, the anti-viral response associated with them are often less productive.

From these results, we propose that neonatal immune response is capable of inducing elements of a successful adult response in the brain, including IFNγ and other Th1-related cytokines, but may struggle with the extensive viral load that is produced in the developing neurons. Neurotropic viruses spread readily in less mature or newly-differentiated neurons, which may pose a greater challenge for viral control and clearance in the developing brain (van den Pol et al., 2002). This notion is supported by the observation that MV-infected neonates exhibit more widespread expression of viral antigen in multiple brain regions prior to T cell infiltration, which suggests that the virus spreads readily in neonatal brain tissue. IFNγ plays multiple roles during a CNS infection; however, the anti-inflammatory effects of IFNγ may be protective in the neonatal brain through modulation of immune cell infiltration. The combination of aggressive viral spread and a modified cytokine profile ultimately poses substantial challenges for the neonatal immune response in the brain.

Supplementary Material

Refer to Web version on PubMed Central for supplementary material.

Acknowledgments

We are very grateful to Dr. Glenn Rall (Fox Chase Cancer Center) for providing the CD46+ transgenic mice, Dr. Emmanuelle Nicolas for the quantitative RT-PCR measles virus data (Fox Chase Cancer Center Real Time PCR facility). We thank Drs. Wilson Meng and Kerry Empey for critical insights and evaluation of the manuscript, and Dr. Zachary B. Zalinger for the qRT-PCR primer sequences.

Funding: This work was supported by the Samuel and Emma Winters Foundation (LOD), the Duquesne University Mylan School of Pharmacy (PG, LOD), and the National Institutes of Health (R15-NS087606-01A1; LOD).

Abbreviations

Abs	Antibodies
ANOVA	Analysis of variance
APC	Allophycocyanin
ATCC	American Type Tissue Collection
BMP	bone morphogenetic protein
CHIKV	Chikungunya virus
CIITA	Class II Major Histocompatibility Complex Transactivator
DPI	days post-infection
FITC	Fluorescein isothiocyanate
Hsp70	Heat shock protein 70
Iba1	Ionized Calcium-Binding Adapter Molecule 1
IFN	Interferon
IFNα	Interferon-alpha
IFNβ	Interferon-beta
IFNγ	Interferon-gamma
KO	Knockout
LACV	La Crosse virus
MV	Measles virus
MDA5	melanoma differentiation-associated gene 5
MHC	Major histocompatibility complex
NK cell	Natural killer cell
NSE	Neuron-specific enolase
N	Nucleocapsid
N.S	Not significant
PRR	Pattern recognition receptors
PFU	Plaque forming unit
PFA	Paraformaldehyde
PE	Phycoerythrin

RIGI	retinoic acid-induced gene-1
RSV	Respiratory syncytial virus
TNF	tumor necrosis factor
TLRs	Toll-like receptors

References

Adkins B, Leclerc C, Marshall-Clarke S. Neonatal adaptive immunity comes of age. Nat Rev Immunol. 2004; 4:553–64. [PubMed: 15229474]

Akira S, Uematsu S, Takeuchi O. Pathogen recognition and innate immunity. Cell. 2006; 124:783–801. [PubMed: 16497588]

An J, Zhou DS, Zhang JL, Morida H, Wang JL, Yasui K. Dengue-specific CD8+ T cells have both protective and pathogenic roles in dengue virus infection. Immunol Lett. 2004; 95:167–74. [PubMed: 15388257]

Basha S, Surendran N, Pichichero M. Immune responses in neonates. Expert Rev Clin Immunol. 2014; 10:1171–84. [PubMed: 25088080]

Biron CA, Nguyen KB, Pien GC, Cousens LP, Salazar-Mather TP. Natural killer cells in antiviral defense: function and regulation by innate cytokines. Annu Rev Immunol. 1999; 17:189–220. [PubMed: 10358757]

Bozic CR, Kolakowski LF Jr, Gerard NP, Garcia-Rodriguez C, von Uexkull-Guldenband C, Conklyn MJ, et al. Expression and biologic characterization of the murine chemokine KC. J Immunol. 1995; 154:6048–57. [PubMed: 7751647]

Brice GT, Graber NL, Hoffman SL, Doolan DL. Expression of the chemokine MIG is a sensitive and predictive marker for antigen-specific, genetically restricted IFN-gamma production and IFN-gamma-secreting cells. J Immunol Methods. 2001; 257:55–69. [PubMed: 11687239]

Burdeinick-Kerr R, Wind J, Griffin DE. Synergistic roles of antibody and interferon in noncytolytic clearance of Sindbis virus from different regions of the central nervous system. J Virol. 2007; 81:5628–36. [PubMed: 17376910]

Callan MF, Steven N, Krausa P, Wilson JD, Moss PA, Gillespie GM, et al. Large clonal expansions of CD8+ T cells in acute infectious mononucleosis. Nat Med. 1996; 2:906–11. [PubMed: 8705861]

Cavanaugh SE, Holmgren AM, Rall GF. Homeostatic interferon expression in neurons is sufficient for early control of viral infection. J Neuroimmunol. 2015; 279:11–9. [PubMed: 25669994]

Chesler DA, Dodard C, Lee GY, Levy DE, Reiss CS. Interferon-gamma-induced inhibition of neuronal vesicular stomatitis virus infection is STAT1 dependent. J Neurovirol. 2004; 10:57–63. [PubMed: 14982729]

Couper KN, Blount DG, Riley EM. IL-10: the master regulator of immunity to infection. J Immunol. 2008; 180:5771–7. [PubMed: 18424693]

Das S, Basu A. Viral infection and neural stem/progenitor cell's fate: implications in brain development and neurological disorders. Neurochem Int. 2011; 59:357–66. [PubMed: 21354238]

Drescher B, Bai F. Neutrophil in viral infections, friend or foe? Virus Res. 2013; 171:1–7. [PubMed: 23178588]

Empey KM, Orend JG, Peebles RS Jr, Egana L, Norris KA, Oury TD, et al. Stimulation of immature lung macrophages with intranasal interferon gamma in a novel neonatal mouse model of respiratory syncytial virus infection. PLoS One. 2012; 7:e40499. [PubMed: 22792355]

Fantetti KN, Gray EL, Ganesan P, Kulkarni A, O'Donnell LA. Interferon gamma protects neonatal neural stem/progenitor cells during measles virus infection of the brain. J Neuroinflammation. 2016; 13:107. [PubMed: 27178303]

Forsthuber T, Yip HC, Lehmann PV. Induction of TH1 and TH2 immunity in neonatal mice. Science. 1996; 271:1728–30. [PubMed: 8596934]

Greter M, Lelios I, Croxford AL. Microglia Versus Myeloid Cell Nomenclature during Brain Inflammation. Front Immunol. 2015; 6:249. [PubMed: 26074918]

Hausmann J, Pagenstecher A, Baur K, Richter K, Rziha HJ, Staeheli P. CD8 T cells require gamma interferon to clear borna disease virus from the brain and prevent immune system-mediated neuronal damage. J Virol. 2005; 79:13509–18. [PubMed: 16227271]

Hayasaka D, Shirai K, Aoki K, Nagata N, Simantini DS, Kitaura K, et al. TNF-alpha acts as an immunoregulator in the mouse brain by reducing the incidence of severe disease following Japanese encephalitis virus infection. PLoS One. 2013; 8:e71643. [PubMed: 23940775]

Jang H, Boltz DA, Webster RG, Smeyne RJ. Viral parkinsonism. Biochim Biophys Acta. 2009; 1792:714–21. [PubMed: 18760350]

Khandaker GM, Zimbron J, Lewis G, Jones PB. Prenatal maternal infection, neurodevelopment and adult schizophrenia: a systematic review of population-based studies. Psychol Med. 2013; 43:239–57. [PubMed: 22717193]

Kim MY, Shu Y, Carsillo T, Zhang J, Yu L, Peterson C, et al. hsp70 and a novel axis of type I interferon-dependent antiviral immunity in the measles virus-infected brain. J Virol. 2013; 87:998–1009. [PubMed: 23135720]

King NJ, Getts DR, Getts MT, Rana S, Shrestha B, Kesson AM. Immunopathology of flavivirus infections. Immunol Cell Biol. 2007; 85:33–42. [PubMed: 17146465]

Komatsu T, Bi Z, Reiss CS. Interferon-gamma induced type I nitric oxide synthase activity inhibits viral replication in neurons. J Neuroimmunol. 1996; 68:101–8. [PubMed: 8784266]

Kopp SJ, Ranaivo HR, Wilcox DR, Karaba AH, Wainwright MS, Muller WJ. Herpes simplex virus serotype and entry receptor availability alter CNS disease in a mouse model of neonatal HSV. Pediatr Res. 2014; 76:528–34. [PubMed: 25198371]

Lambert L, Sagfors AM, Openshaw PJ, Culley FJ. Immunity to RSV in Early-Life. Front Immunol. 2014; 5:466. [PubMed: 25324843]

Landreau F, Galeano P, Caltana LR, Masciotra L, Chertcoff A, Pontoriero A, et al. Effects of two commonly found strains of influenza A virus on developing dopaminergic neurons, in relation to the pathophysiology of schizophrenia. PLoS One. 2012; 7:e51068. [PubMed: 23251423]

Larena M, Regner M, Lobigs M. Cytolytic effector pathways and IFN-gamma help protect against Japanese encephalitis. Eur J Immunol. 2013; 43:1789–98. [PubMed: 23568450]

Lawrence DM, Vaughn MM, Belman AR, Cole JS, Rall GF. Immune response-mediated protection of adult but not neonatal mice from neuron-restricted measles virus infection and central nervous system disease. J Virol. 1999; 73:1795–801. [PubMed: 9971756]

Lee EY, Schultz KL, Griffin DE. Mice deficient in interferon-gamma or interferon-gamma receptor 1 have distinct inflammatory responses to acute viral encephalomyelitis. PLoS One. 2013; 8:e76412. [PubMed: 24204622]

Li L, Lee HH, Bell JJ, Gregg RK, Ellis JS, Gessner A, et al. IL-4 utilizes an alternative receptor to drive apoptosis of Th1 cells and skews neonatal immunity toward Th2. Immunity. 2004; 20:429–40. [PubMed: 15084272]

Licon Luna RM, Lee E, Mullbacher A, Blanden RV, Langman R, Lobigs M. Lack of both Fas ligand and perforin protects from flavivirus-mediated encephalitis in mice. J Virol. 2002; 76:3202–11. [PubMed: 11884544]

Manchester M, Eto DS, Oldstone MB. Characterization of the inflammatory response during acute measles encephalitis in NSE-CD46 transgenic mice. J Neuroimmunol. 1999; 96:207–17. [PubMed: 10337919]

Marr N, Wang TI, Kam SH, Hu YS, Sharma AA, Lam A, et al. Attenuation of respiratory syncytial virus-induced and RIG-I-dependent type I IFN responses in human neonates and very young children. J Immunol. 2014; 192:948–57. [PubMed: 24391215]

McCarthy MK, Procario MC, Twisselmann N, Wilkinson JE, Archambeau AJ, Michele DE, et al. Proinflammatory effects of interferon gamma in mouse adenovirus 1 myocarditis. J Virol. 2015; 89:468–79. [PubMed: 25320326]

Mizuno T, Zhang G, Takeuchi H, Kawanokuchi J, Wang J, Sonobe Y, et al. Interferon-gamma directly induces neurotoxicity through a neuron specific, calcium-permeable complex of IFN-gamma receptor and AMPA GluR1 receptor. FASEB J. 2008; 22:1797–806. [PubMed: 18198214]

Moore KW, de Waal Malefyt R, Coffman RL, O'Garra A. Interleukin-10 and the interleukin-10 receptor. Annu Rev Immunol. 2001; 19:683–765. [PubMed: 11244051]

Muhl H, Pfeilschifter J. Anti-inflammatory properties of pro-inflammatory interferon-gamma. Int Immunopharmacol. 2003; 3:1247–55. [PubMed: 12890422]

Myrick C, DiGuisto R, DeWolfe J, Bowen E, Kappler J, Marrack P, et al. Linkage analysis of variations in CD4:CD8 T cell subsets between C57BL/6 and DBA/2. Genes Immun. 2002; 3:144–50. [PubMed: 12070778]

O'Donnell LA, Conway S, Rose RW, Nicolas E, Slifker M, Balachandran S, et al. STAT1-independent control of a neurotropic measles virus challenge in primary neurons and infected mice. J Immunol. 2012; 188:1915–23. [PubMed: 22246627]

O'Donnell LA, Henkins KM, Kulkarni A, Matullo CM, Balachandran S, Pattisapu AK, et al. Interferon Gamma Induces Protective Non-Canonical Signaling Pathways in Primary Neurons. J Neurochem. 2015

Ottum PA, Arellano G, Reyes LI, Iruretagoyena M, Naves R. Opposing Roles of Interferon-Gamma on Cells of the Central Nervous System in Autoimmune Neuroinflammation. Front Immunol. 2015; 6:539. [PubMed: 26579119]

Paolini R, Bernardini G, Molfetta R, Santoni A. NK cells and interferons. Cytokine Growth Factor Rev. 2015; 26:113–20. [PubMed: 25443799]

Patterson CE, Lawrence DM, Echols LA, Rall GF. Immune-mediated protection from measles virus-induced central nervous system disease is noncytolytic and gamma interferon dependent. J Virol. 2002; 76:4497–506. [PubMed: 11932415]

Phares TW, Stohlman SA, Hwang M, Min B, Hinton DR, Bergmann CC. CD4 T cells promote CD8 T cell immunity at the priming and effector site during viral encephalitis. J Virol. 2012; 86:2416–27. [PubMed: 22205741]

Pott J, Stockinger S, Torow N, Smoczek A, Lindner C, McInerney G, et al. Age-dependent TLR3 expression of the intestinal epithelium contributes to rotavirus susceptibility. PLoS Pathog. 2012; 8:e1002670. [PubMed: 22570612]

Powell TJ Jr, Streilein JW. Neonatal tolerance induction by class II alloantigens activates IL-4-secreting, tolerogen-responsive T cells. J Immunol. 1990; 144:854–9. [PubMed: 2136901]

Rall GF, Manchester M, Daniels LR, Callahan EM, Belman AR, Oldstone MB. A transgenic mouse model for measles virus infection of the brain. Proc Natl Acad Sci U S A. 1997; 94:4659–63. [PubMed: 9114047]

Reith W, LeibundGut-Landmann S, Waldburger JM. Regulation of MHC class II gene expression by the class II transactivator. Nat Rev Immunol. 2005; 5:793–806. [PubMed: 16200082]

Rock RB, Hu S, Deshpande A, Munir S, May BJ, Baker CA, et al. Transcriptional response of human microglial cells to interferon-gamma. Genes Immun. 2005; 6:712–9. [PubMed: 16163375]

Rouse BT, Sehrawat S. Immunity and immunopathology to viruses: what decides the outcome? Nat Rev Immunol. 2010; 10:514–26. [PubMed: 20577268]

Rudd PA, Wilson J, Gardner J, Larcher T, Babarit C, Le TT, et al. Interferon response factors 3 and 7 protect against Chikungunya virus hemorrhagic fever and shock. J Virol. 2012; 86:9888–98. [PubMed: 22761364]

Ryman KD, Gardner CL, Meier KC, Biron CA, Johnston RE, Klimstra WB. Early restriction of alphavirus replication and dissemination contributes to age-dependent attenuation of systemic hyperinflammatory disease. J Gen Virol. 2007; 88:518–29. [PubMed: 17251570]

Sasaki Y, Ohsawa K, Kanazawa H, Kohsaka S, Imai Y. Iba1 is an actin-cross-linking protein in macrophages/microglia. Biochem Biophys Res Commun. 2001; 286:292–7. [PubMed: 11500035]

Schneider WM, Chevillotte MD, Rice CM. Interferon-stimulated genes: a complex web of host defenses. Annu Rev Immunol. 2014; 32:513–45. [PubMed: 24555472]

Schoenborn JR, Wilson CB. Regulation of interferon-gamma during innate and adaptive immune responses. Adv Immunol. 2007; 96:41–101. [PubMed: 17981204]

Singh RR, Hahn BH, Sercarz EE. Neonatal peptide exposure can prime T cells and, upon subsequent immunization, induce their immune deviation: implications for antibody vs. T cell-mediated autoimmunity. J Exp Med. 1996; 183:1613–21. [PubMed: 8666919]

Slavica L, Nordstrom I, Karlsson MN, Valadi H, Kacerovsky M, Jacobsson B, et al. TLR3 impairment in human newborns. J Leukoc Biol. 2013; 94:1003–11. [PubMed: 23901120]

Solomos AC, O'Regan KJ, Rall GF. CD4+ T cells require either B cells or CD8+ T cells to control spread and pathogenesis of a neurotropic infection. Virology. 2016; 499:196–202. [PubMed: 27677156]

Sorgeloos F, Kreit M, Hermant P, Lardinois C, Michiels T. Antiviral type I and type III interferon responses in the central nervous system. Viruses. 2013; 5:834–57. [PubMed: 23503326]

Stifter SA, Bhattacharyya N, Pillay R, Florido M, Triccas JA, Britton WJ, et al. Functional Interplay between Type I and II Interferons Is Essential to Limit Influenza A Virus-Induced Tissue Inflammation. PLoS Pathog. 2016; 12:e1005378. [PubMed: 26731100]

Stout-Delgado HW, Du W, Shirali AC, Booth CJ, Goldstein DR. Aging promotes neutrophil-induced mortality by augmenting IL-17 production during viral infection. Cell Host Microbe. 2009; 6:446–56. [PubMed: 19917499]

Stubblefield Park SR, Widness M, Levine AD, Patterson CE. T cell-, interleukin-12-, and gamma interferon-driven viral clearance in measles virus-infected brain tissue. J Virol. 2011; 85:3664–76. [PubMed: 21270150]

Sturge CR, Benson A, Raetz M, Wilhelm CL, Mirpuri J, Vitetta ES, et al. TLR-independent neutrophil-derived IFN-gamma is important for host resistance to intracellular pathogens. Proc Natl Acad Sci U S A. 2013; 110:10711–6. [PubMed: 23754402]

Tanabe M, Kurita-Taniguchi M, Takeuchi K, Takeda M, Ayata M, Ogura H, et al. Mechanism of up-regulation of human Toll-like receptor 3 secondary to infection of measles virus-attenuated strains. Biochem Biophys Res Commun. 2003; 311:39–48. [PubMed: 14575692]

Taylor KG, Woods TA, Winkler CW, Carmody AB, Peterson KE. Age-dependent myeloid dendritic cell responses mediate resistance to la crosse virus-induced neurological disease. J Virol. 2014; 88:11070–9. [PubMed: 25008929]

Tishon A, Lewicki H, Andaya A, McGavern D, Martin L, Oldstone MB. CD4 T cell control primary measles virus infection of the CNS: regulation is dependent on combined activity with either CD8 T cells or with B cells: CD4, CD8 or B cells alone are ineffective. Virology. 2006; 347:234–45. [PubMed: 16529787]

Trandem K, Jin Q, Weiss KA, James BR, Zhao J, Perlman S. Virally expressed interleukin-10 ameliorates acute encephalomyelitis and chronic demyelination in coronavirus-infected mice. J Virol. 2011a; 85:6822–31. [PubMed: 21593179]

Trandem K, Zhao J, Fleming E, Perlman S. Highly activated cytotoxic CD8 T cells express protective IL-10 at the peak of coronavirus-induced encephalitis. J Immunol. 2011b; 186:3642–52. [PubMed: 21317392]

Tripp RA, Hou S, McMickle A, Houston J, Doherty PC. Recruitment and proliferation of CD8+ T cells in respiratory virus infections. J Immunol. 1995; 154:6013–21. [PubMed: 7751644]

Trujillo JA, Fleming EL, Perlman S. Transgenic CCL2 expression in the central nervous system results in a dysregulated immune response and enhanced lethality after coronavirus infection. J Virol. 2013; 87:2376–89. [PubMed: 23269787]

Tun MM, Aoki K, Senba M, Buerano CC, Shirai K, Suzuki R, et al. Protective role of TNF-alpha, IL-10 and IL-2 in mice infected with the Oshima strain of Tick-borne encephalitis virus. Sci Rep. 2014; 4:5344. [PubMed: 24938868]

van den Pol AN, Reuter JD, Santarelli JG. Enhanced cytomegalovirus infection of developing brain independent of the adaptive immune system. J Virol. 2002; 76:8842–54. [PubMed: 12163604]

Willenborg DO, Fordham SA, Staykova MA, Ramshaw IA, Cowden WB. IFN-gamma is critical to the control of murine autoimmune encephalomyelitis and regulates both in the periphery and in the target tissue: a possible role for nitric oxide. J Immunol. 1999; 163:5278–86. [PubMed: 10553050]

Yoneyama M, Kikuchi M, Natsukawa T, Shinobu N, Imaizumi T, Miyagishi M, et al. The RNA helicase RIG-I has an essential function in double-stranded RNA-induced innate antiviral responses. Nat Immunol. 2004; 5:730–7. [PubMed: 15208624]

Zaghouani H, Hoeman CM, Adkins B. Neonatal immunity: faulty T-helpers and the shortcomings of dendritic cells. Trends Immunol. 2009; 30:585–91. [PubMed: 19846341]

Zalinger ZB, Elliott R, Rose KM, Weiss SR. MDA5 Is Critical to Host Defense during Infection with Murine Coronavirus. J Virol. 2015; 89:12330–40. [PubMed: 26423942]

Highlights

- The role of the anti-viral cytokine interferon-gamma (IFNγ) is investigated during a neonatal viral infection in CNS neurons
- IFNγ did not prevent mortality in neonates, but it slowed disease progression and reduced neutrophil, macrophage, and T cell infiltration
- Both adult and neonatal mice expressed Th1-like cytokines, including IFNγ and some IFNγ-stimulated genes, during infection
- Despite a Th1-like cytokine profile in the neonatal CNS, the cytokine milieu is ultimately ineffective at controlling viral spread

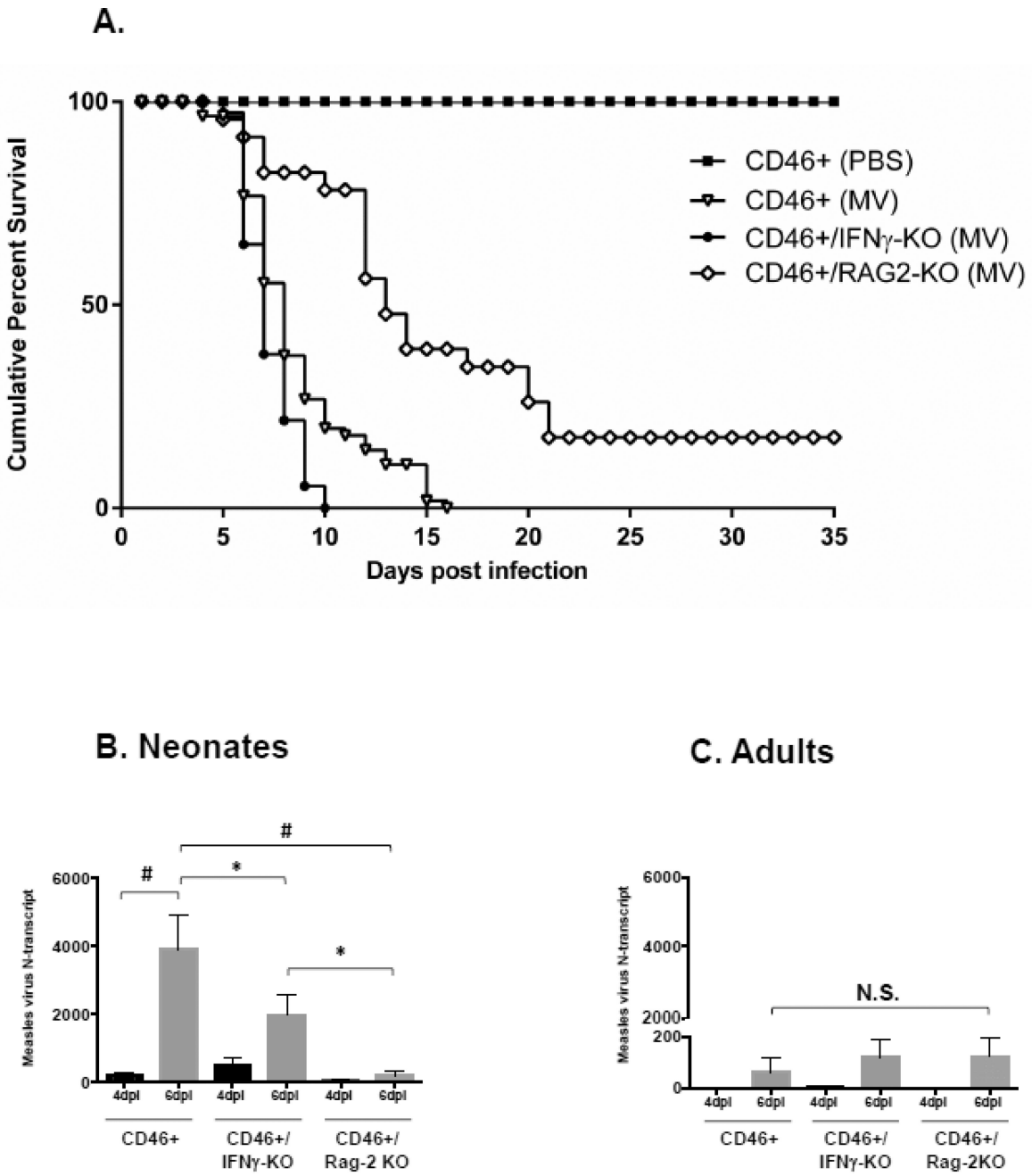

Figure 1. IFNγ delays, but does not prevent, mortality despite higher viral load in infected CD46+ neonates

A. Kaplan-Meier plot of CD46+ neonates on various knockout backgrounds. CD46+, CD46+/IFNγ-KO, and CD46+/RAG2-KO neonates were infected intracranially with measles virus (MV) (10^4 PFU/10μl PBS) at 2 days of age. Mice were monitored for symptoms of illness and death for 35 days post-infection. Statistical analysis was applied by log rank test ($p < 0.0001$). Results from 4–6 separate litters were pooled ($n = 30–50$ mice per condition). Whole brain lysates from neonatal (B) and adult (C) MV-infected mice were collected at 4 and 6 dpi. RNA levels of measles virus nucleocapsid (N) transcript were quantified using qRT-PCR. Bars represent the average of mice from three independent

experiments (n=9–14) and error bars represent SD. Statistical analysis was applied by two-way ANOVA (# $p<0.001$, * $p<0.05$, NS = not significant) with Bonferroni post hoc test.

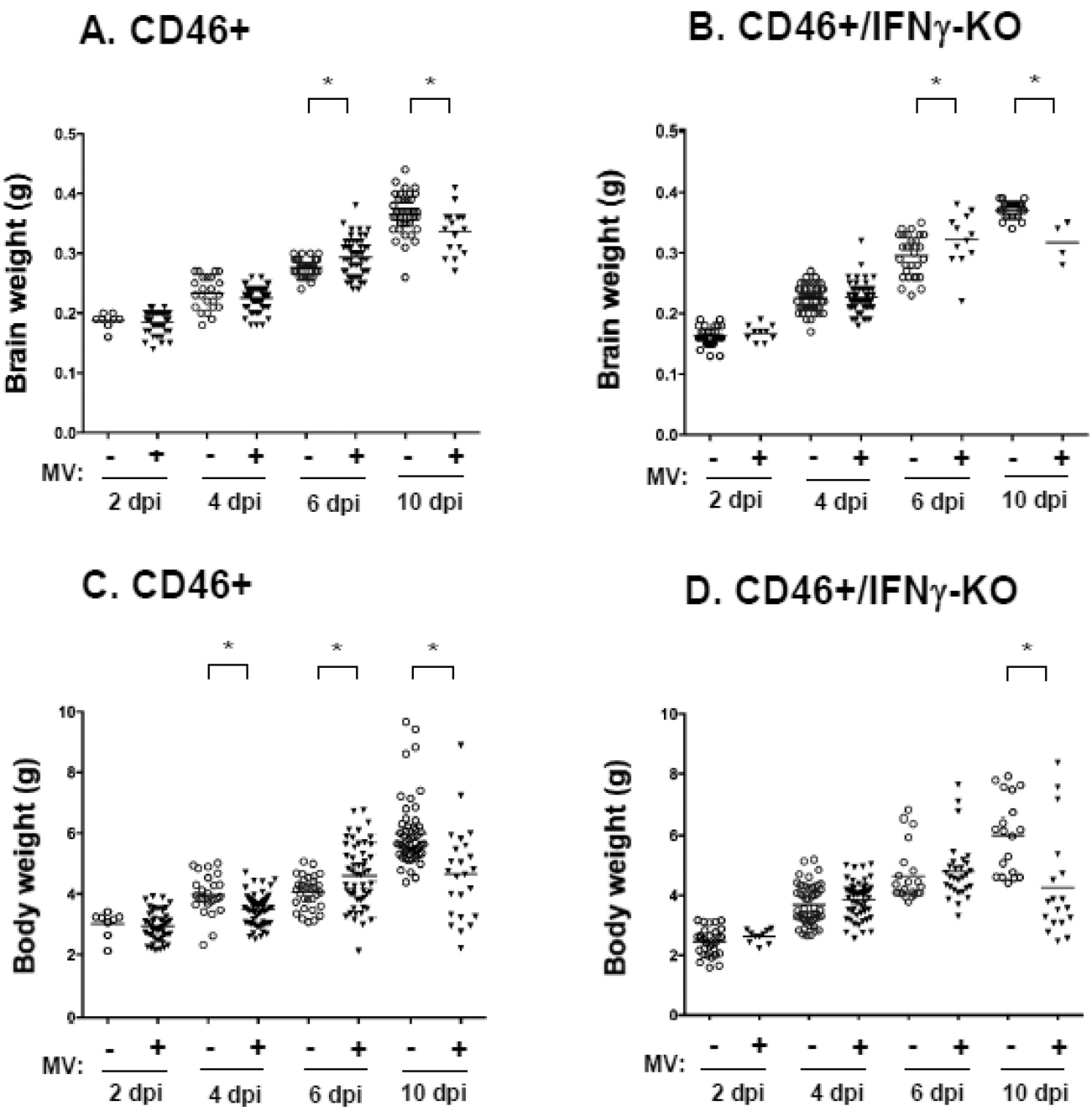

Figure 2. CD46+ neonates lose body and brain weight at early and late time points post-infection

The body weights (A, B) and brain weights (C, D) of CD46+ (A, C) and CD46+/IFNγ-KO neonates (B, D) at different time points post-infection were measured. Weights were recorded at the time of harvest for flow cytometry experiments. Mean values are represented by horizontal bars for each condition. Statistical analysis was applied by two-way ANOVA (* $p<0.05$) with Bonferroni post hoc test.

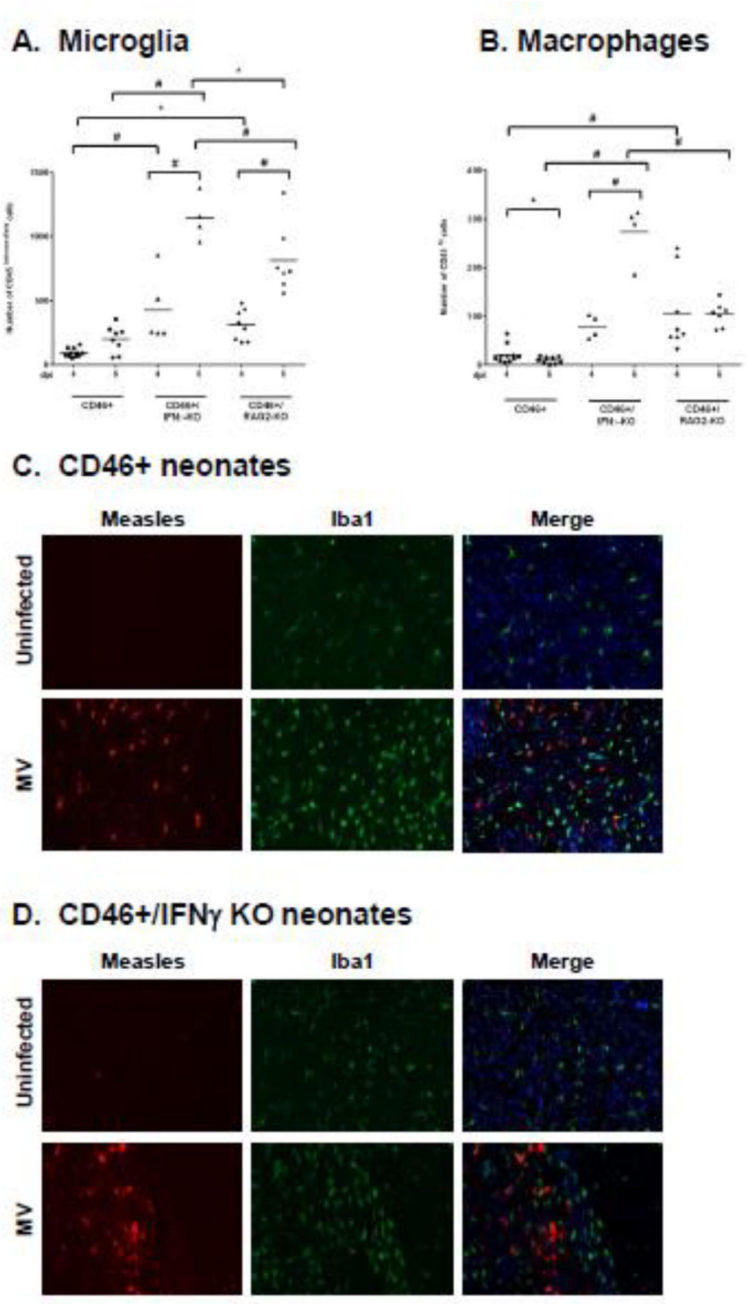

Figure 3. Infiltration of macrophages and activation of microglia in the CNS occurs during MV-infection in an IFNγ-independent manner

Whole brain homogenates from CD46+ (A) and CD46+/IFNγ-KO (B) neonates were analyzed for microglia (A; $CD45^{intermediate}$) and macrophages (B; $CD45^{high}$) by flow cytometry. The horizontal line represents the mean number of cells for each condition. Results from 4–5 different litters were collected, and statistical analysis was applied by two-way ANOVA (# $p<0.001$, * $p<0.05$) with Bonferroni post hoc test. Whole brains from MV-infected and uninfected control CD46+ neonates (C) and CD46+/IFNγ-KO neonates (D) were collected at 7 dpi. Sagittal sections from the neocortex were immunostained for measles (Hemagglutinin and Matrix protein; red), microglia/macrophages (Iba1; green) and

Hoechst 33342 stain (blue) as a nuclear marker. Slides from 4–5 mice per condition were examined, and representative sections with MV+ cells are shown. Scale bar = 200μm

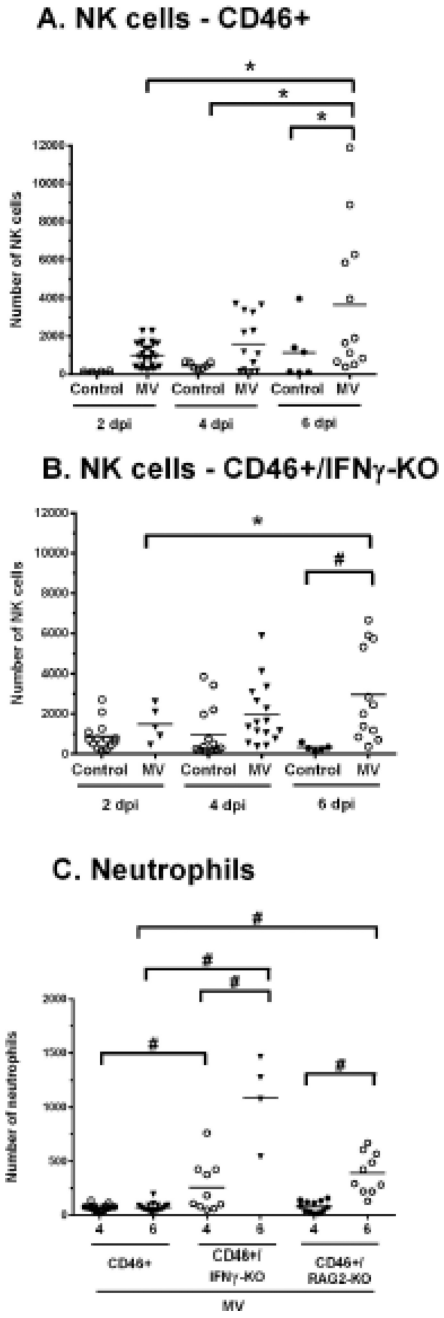

Figure 4. IFNγ does not affect NK cell infiltration, but downregulates neutrophil infiltration, in neonates

Whole brain homogenates from CD46+ (A) and CD46+/IFNγ-KO (B) neonates were analyzed for total natural killer (NK) cell numbers at 2, 4, and 6 dpi by flow cytometry (CD3-/NK1.1+/CD49b+). The horizontal line represents the mean number of cells for each condition. Results from 4–5 different litters were collected, and statistical analysis was applied by two-way ANOVA (# $p<0.001$, * $p<0.05$) with Bonferroni post hoc test. Whole brain homogenates from MV-infected CD46+, CD46+/IFNγ-KO, and CD46+/RAG2-KO neonates (C) were analyzed for neutrophils numbers ($CD45^{hi}$/CD11b+/Ly6G+) at 4 dpi and

6dpi by flow cytometry. Results from 3 different litters were collected, and statistical analysis was applied by one-way ANOVA (* $p<0.05$) with Bonferroni post hoc test.

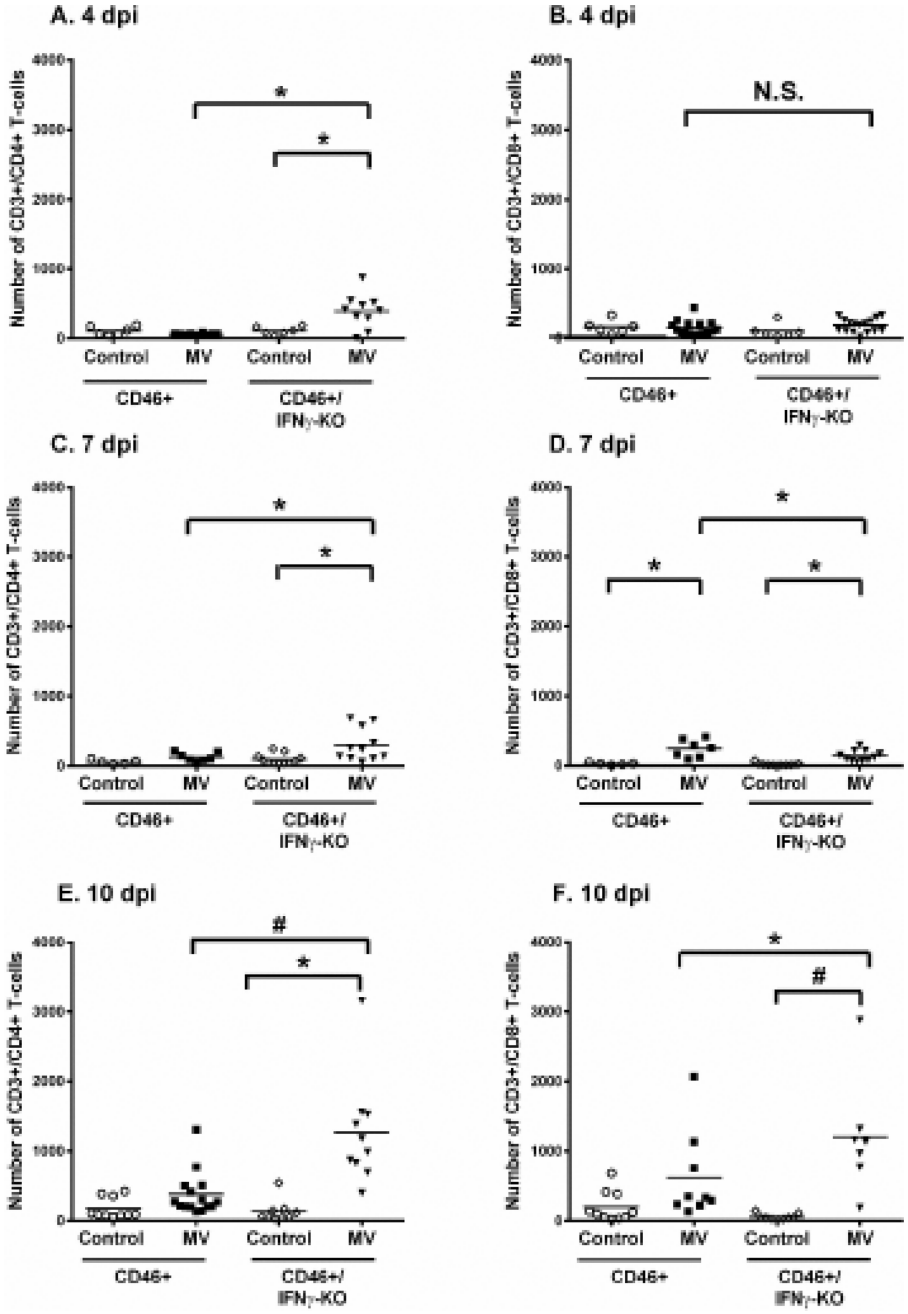

Figure 5. Neonates show higher T cell infiltration at later stages of infection in the absence of IFNγ

Flow cytometry was performed on whole brain homogenates for CD4 T cells (CD3+/CD4+/CD19-) or CD8 T cells (CD3+/CD8+/CD19-). CD4 T-cells (left column; A, C, E) and CD8 T cells (right column; B, D, E) were quantified in uninfected and MV-infected CD46+ and CD46+/IFNγ-KO neonates at 4 (A, B), 7 (C, D), and 10 dpi (E, F). The black line represents the mean number of cells for each group. Results represent pups from 4–5 different litters. Statistical analysis was applied by two-way ANOVA (* $p<0.05$, # $p<0.001$) with Bonferroni post hoc test.

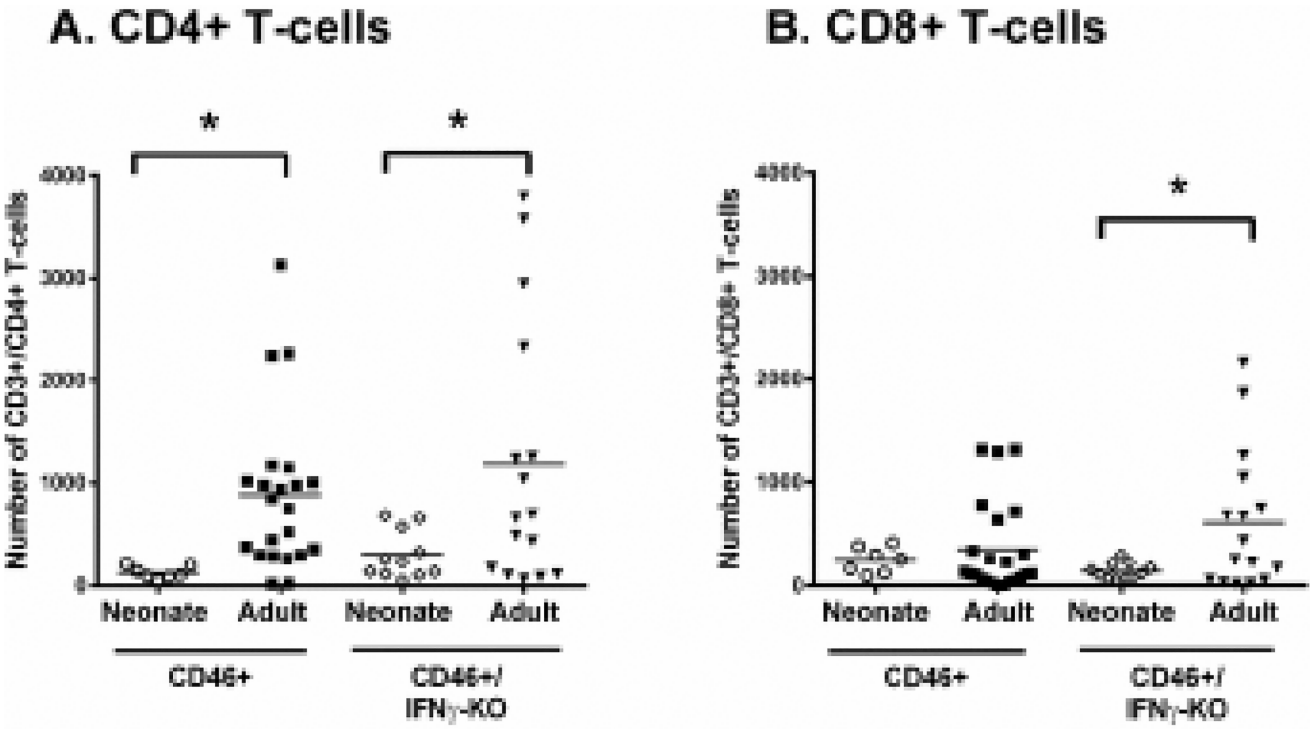

Figure 6. CD4 T cell infiltration in the CNS is greater in MV-infected adults than in neonates

Whole brain homogenates from neonatal and adult CD46+ (A) and CD46+/IFNγ-KO (B) mice were analyzed for infiltrating T cells at 7 dpi. Flow cytometry was performed for CD4 T cells (CD3+/CD4+/CD19-) or CD8 T cells (CD3+/CD8+/CD19-). Mice from 4–5 different litters were compared for each condition. Statistical analysis was applied by two-way ANOVA (* $p<0.05$) with Bonferroni post hoc test.

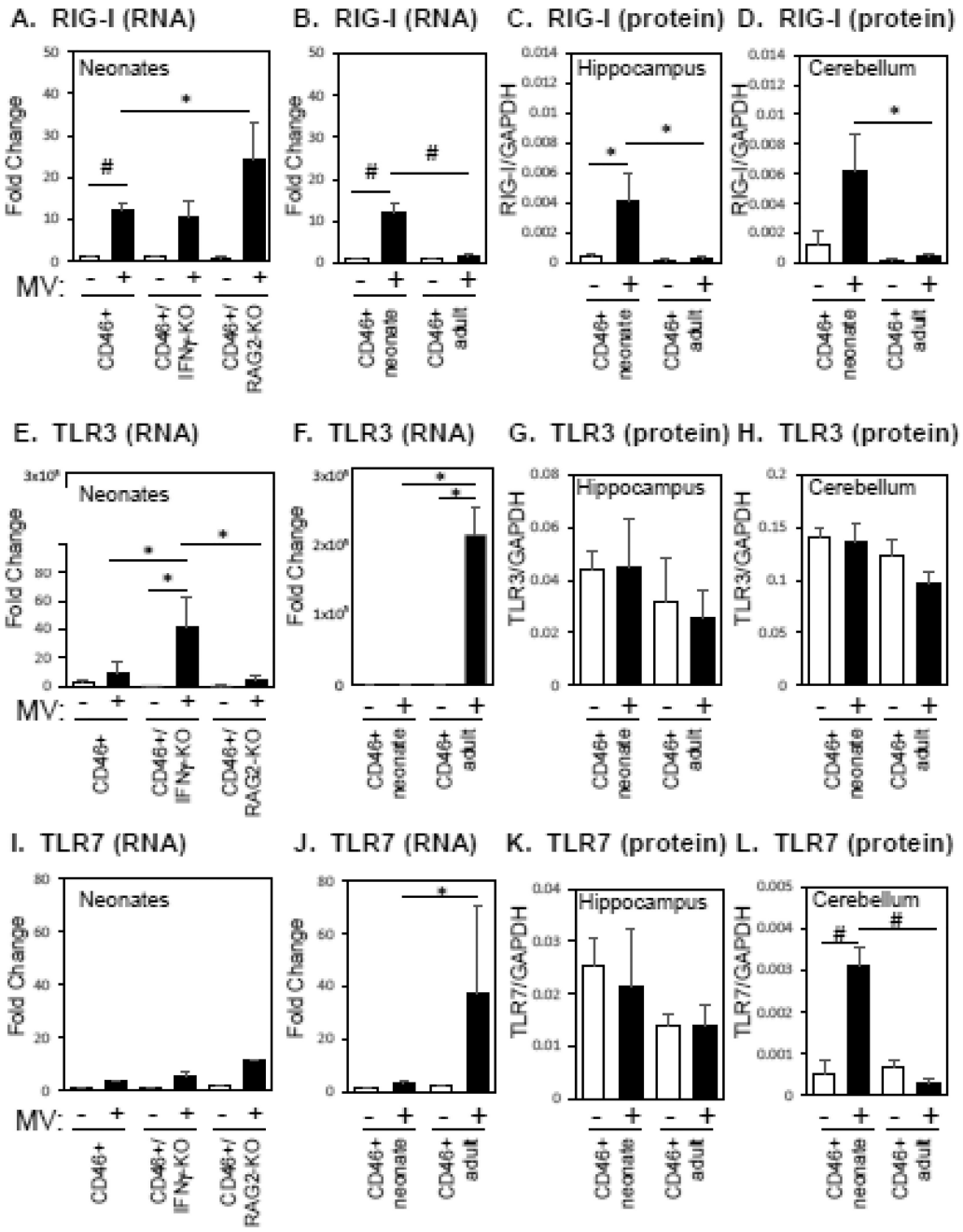

Figure 7. MV-infection induces distinct expression of pattern recognition receptors in the neonatal and adult CNS

Brains of uninfected and MV-infected CD46+ mice were analyzed for the mRNA and protein expression of pattern recognition receptors (PRRs) at 7 dpi. CD46+, CD46+/IFNγ-KO, and CD46+/RAG2-KO neonates (first column) or CD46+ neonates and adults (second, third, and fourth columns) were compared. qRT-PCR analysis of the whole brain was performed for RIGI (A, B), TLR3 (E, F), and TLR7 (I, J). mRNA expression is shown as the fold-change normalized to the CD46+ uninfected controls (n=4–5 mice/condition). Lysates of hippocampal (C, G, K) and cerebellar (D, H, L) tissue were analyzed by western blots for RIG-I (C, D), TLR3 (G, H), and TLR7 (K, L). Protein expression is shown as the

fluorescence signal for each protein quantified and normalized to GAPDH (n=3–4 mice/condition). Each bar represents the mean fold-change and SEM. Statistical differences were determined by two-way ANOVA (* $p<0.05$, # $p<0.001$) with Bonferroni post hoc test.

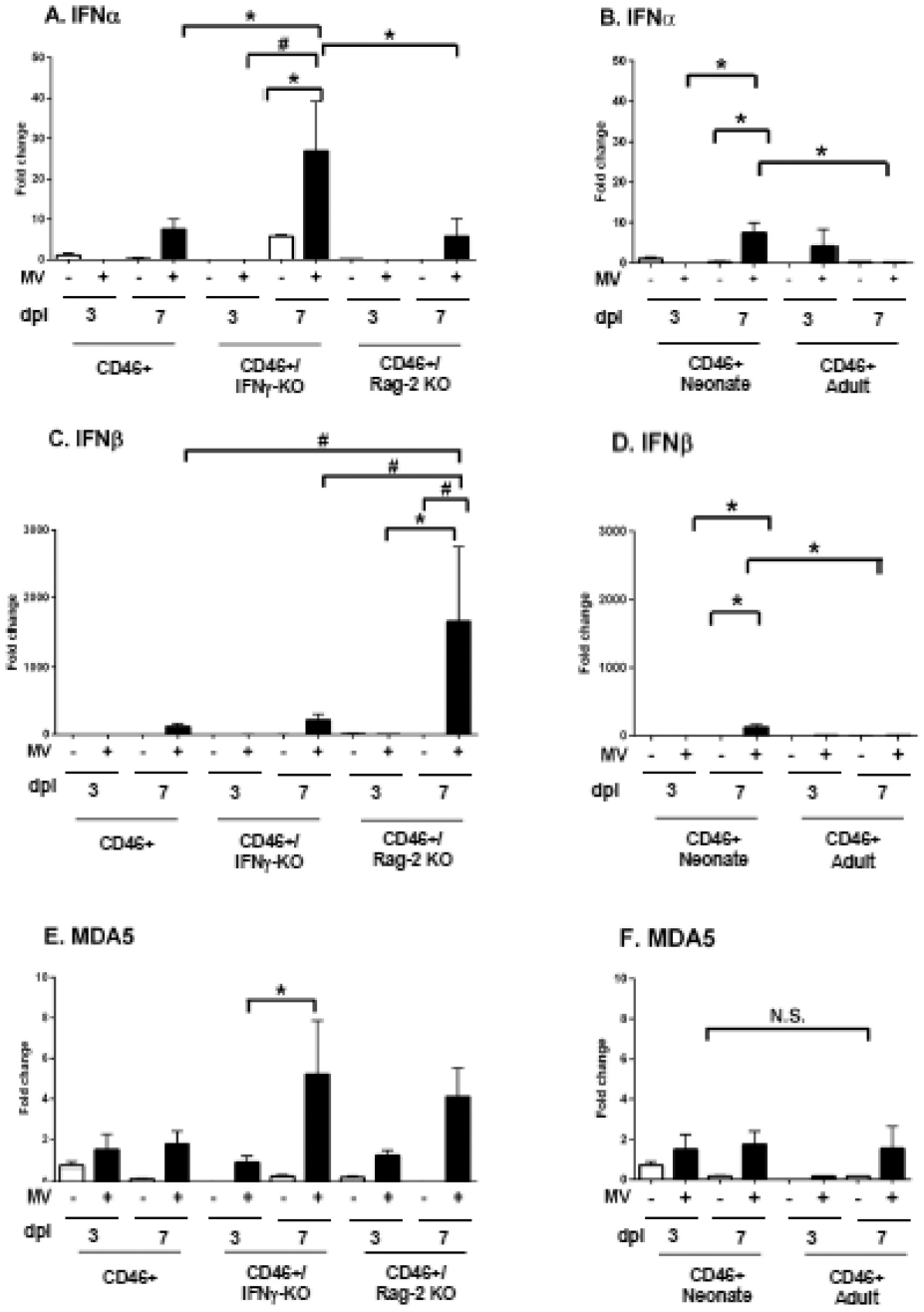

Figure 8. Neonatal mice induce greater expression of Type I interferons during MV infection in comparison to adults

Brains of uninfected and MV-infected CD46+ mice were analyzed for the mRNA expression of Type I interferons at 3 dpi and 7 dpi. CD46+, CD46+/IFNγ-KO, and CD46+/RAG2-KO neonates (left column; A, C, E) and CD46+ neonates and adults (right column; B, D, F) were compared. qRT-PCR analysis was performed for IFNα4 (A, B), IFNβ (C, D) and MDA5 (E, F). Relative gene expression is shown as the fold-change normalized to the CD46+ uninfected controls (n=4–5 mice/condition). Each bar represents the mean fold-change and SEM. Statistical differences were determined by three-way ANOVA (* $p<0.05$, # $p<0.001$) with Bonferroni post hoc test.

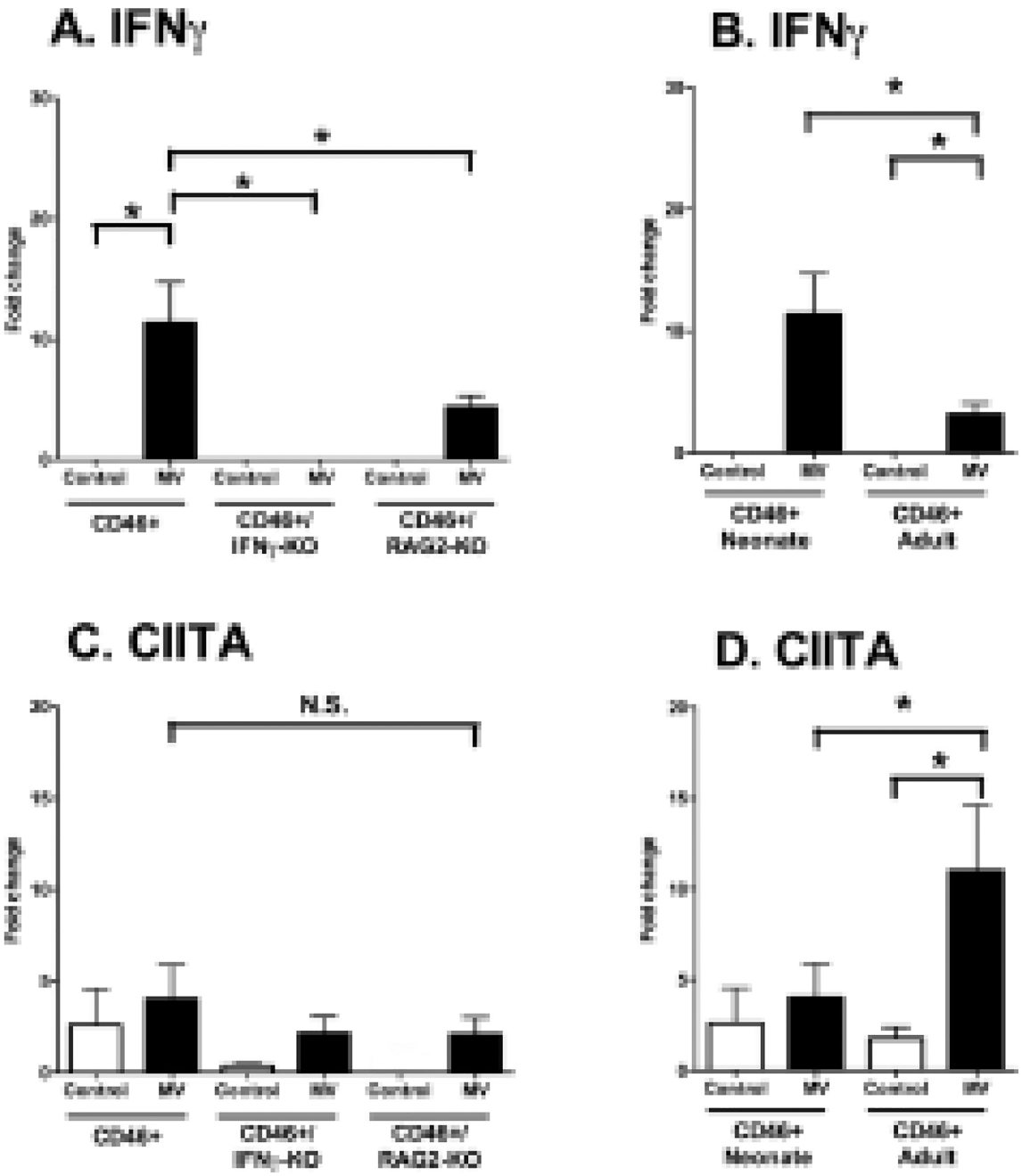

Figure 9. Despite elevated IFNγ expression during infection, transcription of IFNγ-responsive genes is age-dependent

Brains of uninfected and MV-infected CD46+ mice were analyzed for the mRNA expression of IFNγ and CIITA at 7 dpi. CD46+, CD46+/IFNγ-KO, and CD46+/RAG2-KO neonates (left column; A, C) and CD46+ neonates and adults (right column, B, D) were compared. qRT-PCR analysis was performed for IFNγ (A, B) and CIITA (C, D). Relative gene expression is shown as the fold-change normalized to the CD46+ uninfected controls (n=4–5 mice/condition). Each bar represents the mean fold-change and SEM. Statistical differences were determined by two-way ANOVA (* $p<0.05$, # $p<0.001$) with Bonferroni post hoc test.

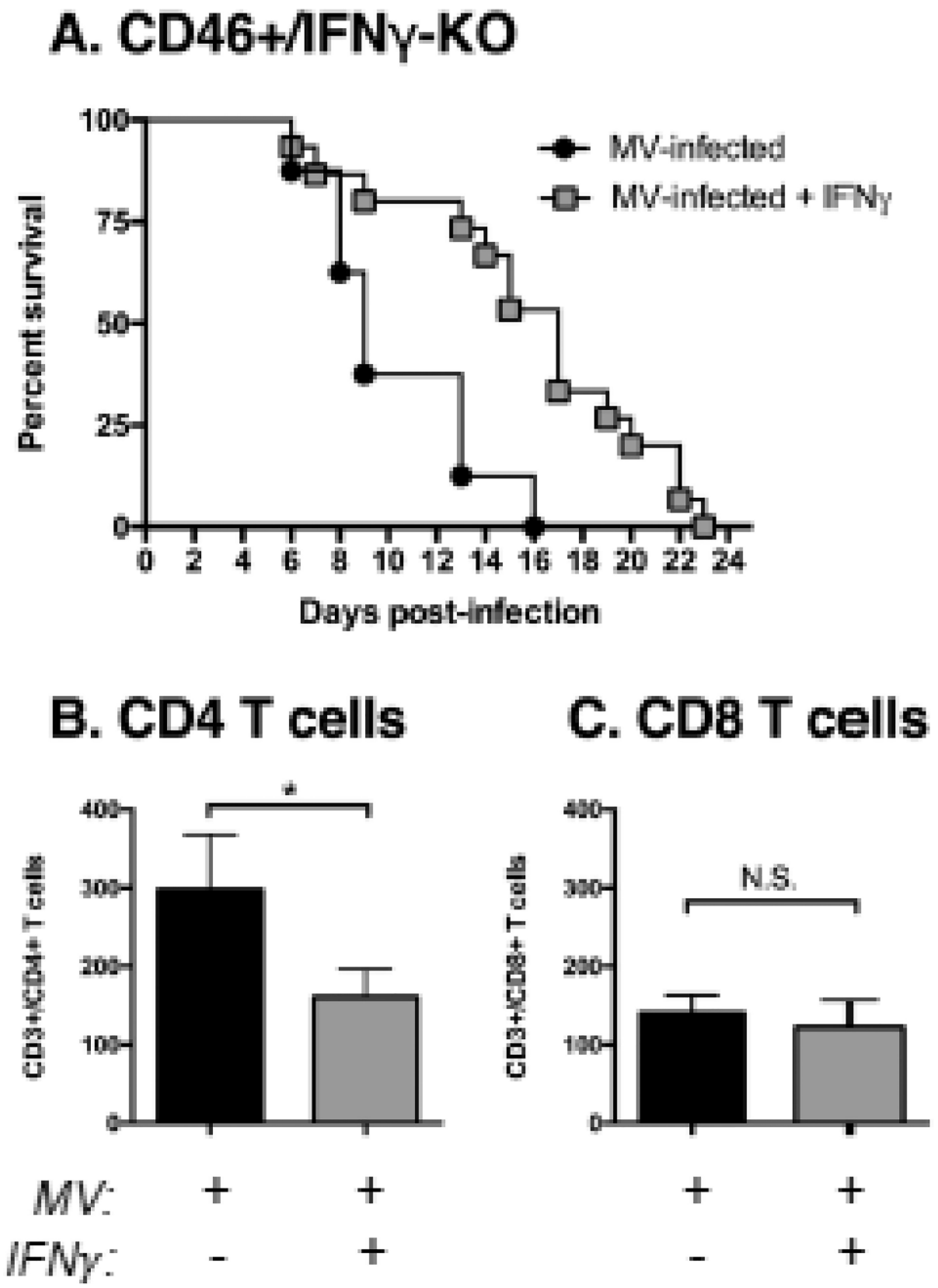

Figure 10. IFNγ delays mortality and reduces CD4 T cell infiltration in CD46+/IFNγ-KO neonates

Kaplan-Meier plot of CD46+/IFNγ-KO neonates infected intracranially with measles virus (MV) (10^4 PFU/10μl PBS) at 2 days of age and treated with recombinant IFNγ (100U in 10μl PBS at the start of infection and every three days post-infection). Mice were monitored for symptoms of illness and death until all mice had succumbed to infection. Statistical analysis was applied by log rank test ($p < 0.01$). Results from two separate litters were pooled (n = 7–10 mice per condition). Whole brain homogenates were analyzed by flow cytometry for CD4 T cells (A; CD3+/CD4+/CD19-) or CD8 T cells (B; CD3+/CD8+/CD19-) at 7 dpi from untreated (black bars) and IFNγ-treated (grey bars) CD46+/IFNγ-KO

neonates infected with MV. Mice from 3–5 different litters were compared for each condition. Each bar represents the average number of T cells per 1×10^5 events and the error bars represent SEM. Statistical differences were determined by student t-test (* $p<0.05$,# $p<0.001$).

Table 1

Gene expression of pro- and anti-inflammatory cytokines in MV-infected neonatal and adult brains

Gene expression of cytokines and chemokines in measles virus-infected neonatal and adult brains. Brain tissue from uninfected and MV-infected CD46+ neonates and adults were collected for RNA extraction at 7 dpi. qRT-PCR array analysis was performed using the RT^2 Profiler™ PCR Array. Changes in the gene expression that were more than two-fold relative to the uninfected controls are shown. All data were normalized against levels of housekeeping genes within the same sample.

		CD46+ Neonate		CD46+ Adult	
Gene	**Description**	**Fold change**	**p-value**	**Fold change**	**p-value**
Cxcl10	Chemokine (C-X-C motif) ligand 10	84.62	0.011	44.43	0.049
IL1rn	Interleukin 1 receptor antagonist	17.84	0.016	14.4	0.025
Ccl5	Chemokine (C-C motif) ligand 5	15.18	0.007	10.84	0.016
IFNγ	Interferon gamma	11.08	0.027	8.1	0.021
Ccl4	Chemokine (C-C motif) ligand 4	10.54	0.012	5.03	0.026
Ccl12	Chemokine (C-C motif) ligand 12	5.69	0.032	15.91	0.011
Cxcl13	Chemokine (C-X-C motif) ligand 13	3.89	0.029	19.18	0.033
Ccl3	Chemokine (C-C motif) ligand 3	3.73	0.021	3.22	0.0003
IL1β	Interleukin 1 beta	3.27	0.027	3.04	0.014
Ccl2	Chemokine (C-C motif) ligand 2	15.33	0.042		
Ccl7	Chemokine (C-C motif) ligand 7	9.31	0.017		
Tnf	Tumor necrosis factor	8.36	0.016		
IL12b	Interleukin 12B	7.87	0.02		
Osm	Oncostatin M	4.44	0.009		
Xcl1	Chemokine (C motif) ligand 1	3.84	0.03		
IL27	Interleukin 27	3.4	0.031		
Cxcl11	Chemokine (C-X-C motif) ligand 11	2.58	0.025		
IL10	Interleukin 10	2.36	0.03		
Cxcl9	Chemokine (C-X-C motif) ligand 9			17.67	0.02
Ccl11	Chemokine (C-X-C motif) ligand 11			2.67	0.002
IL1α	Interleukin 1 alpha			2.67	0.021
Cxcl16	Chemokine (C-X-C motif) ligand 16			2.43	0.01

Gene	Description	CD46+ Neonate		CD46+ Adult	
		Fold change	p-value	Fold change	p-value
Ccl22	Chemokine (C-C motif) ligand 22			2.27	0.039
Tnfsf10	TNF (ligand) superfamily, member 10			2.26	0.038
Fasl	Fas ligand (TNF superfamily, member 6)			2.14	0.015
IL7	Interleukin 7			2.18	0.046

* $p < 0.05$ by students t-test.

Table 2

Gene expression of pro- and anti-inflammatory cytokines in immunocompetent and immunocompromised neonates

Gene expression of cytokines and chemokine in measles virus-infected CD46+, CD46+/IFNγ-KO and CD46+/RAG2-KO neonates. Brain tissue was collected from uninfected and infected neonates and RNA was extracted at 7 dpi. qRT-PCR array analysis was performed using the RT^2 Profiler™ PCR Array. Changes in the gene expression that were more than two-fold relative to the uninfected controls are shown. All data were normalized against levels of housekeeping genes within the same sample.

		CD46+ neonate		CD46+/IFNγ-KO neonate		CD46+/RAG2-KO neonate	
Gene	**Description**	**Fold change**	**p-value**	**Fold change**	**p-value**	**Fold change**	**p-value**
Cxcl10	Chemokine (C-X-C motif) ligand 10	84.62	0.011	291.38	0.001	771.13	0.023
IL1rn	Interleukin 1 receptor antagonist	17.84	0.016	68.96	0.003	214.9	0.0008
Ccl5	Chemokine (C-C motif) ligand 5	15.18	0.007	33.49	0.013	132.97	0.013
IFNγ	Interferon gamma	11.08	0.027	-	-	15.02	0.023
Ccl4	Chemokine (C-C motif) ligand 4	10.54	0.012	32.55	0.007	153.19	0.0001
Ccl12	Chemokine (C-C motif) ligand 12	5.69	0.032	-	-	272.95	0.001
Cxcl13	Chemokine (C-X-C motif) ligand 13	3.89	0.029	14.11	0.016	41.24	0.006
Ccl3	Chemokine (C-C motif) ligand 3	3.73	0.021	8.35	0.003	31.05	0.0001
IL1β	Interleukin 1 beta	3.27	0.027	5.9	0.003	9.85	0.005
Ccl2	Chemokine (C-C motif) ligand 2	15.33	0.042	35.89	0.018	493.99	0.001
Ccl7	Chemokine (C-C motif) ligand 7	9.31	0.017	16.46	0.024	164.18	0.024
Tnf	Tumor necrosis factor	8.36	0.016	17.9	0.007	72.05	0.009
IL12b	Interleukin 12B	7.87	0.02	15.28	0.008	199.93	0.03
Osm	Oncostatin M	4.44	0.009	5.58	0.024	11.29	0.023
Xcl1	Chemokine (C motif) ligand 1	3.84	0.03	13.98	0.009	21.72	0.047
IL27	Interleukin 27	3.4	0.031	6.49	0.001	14.55	0.005
Cxcl11	Chemokine (C-X-C motif) ligand 11	2.58	0.025	5.23	0.007	17	0.018
IL10	Interleukin 10	2.36	0.03	-	-	-	-
Cxcl9	Chemokine (C-X-C motif) ligand 9			9.08	0.004	71.63	0.008
IL6	Interleukin 6			4.77	0.009	16.85	0.004
B2m	beta 2 microglobulin			4.49	0.002	11.86	0.024
IL1α	Interleukin 1 alpha			3.56	0.0003	3.66	0.021

Gene	Description	CD46+ neonate	CD46+/IFNγ-KO neonate		CD46+/RAG2-KO neonate	
		Fold change p-value	Fold change	p-value	Fold change	p-value
CXCL1	Chemokine (C_X_C) ligand 1		2.26	0.036	-	-
Ccl11	Chemokine (C-X-C motif) ligand 11				11.17	0.012
Cxcl16	Chemokine (C-X-C motif) ligand 16				7.23	0.0001
CSF1	Colony stimulating factor 1				6.92	0.0001
IL15	Interleukin 15				6.12	0.0009
Ccl22	Chemokine (C-C motif) ligand 22				6.18	0.012
Ccl19	Chemokine (C-C motif) ligand 19				5.75	0.0001
Tnfsf10	TNF (ligand) superfamily, member 10				5.55	0.0002
IL5	Interleukin 5				3.68	0.03
Ccl17	Chemokine (C-C motif) ligand 17				3.56	0.04
CNTF	Ciliary neurotrophic factor				3.31	0.008
IL3	Interleukin 3				3.09	0.04
Tnfsf13b	TNF (ligand) superfamily, member 13b				2.43	0.045
IL7	Interleukin 7				2.34	0.046
Bmp7	Bone morphogenetic protein 7				3.9	0.02
Bmp6	Bone morphogenetic protein 6				3.4	0.004
Bmp4	Bone morphogenetic protein 4				3	0.024
Bmp2	Bone morphogenetic protein 2				2.85	0.036
Mstn	Myostatin				2.52	0.029

* $p < 0.05$ by students t-test.